SALL1 modulates CBX4 stability, nuclear bodies and regulation of target genes

Immacolata Giordano, Lucia Pirone, Veronica Muratore, Eukene Landaluze, Coralia Pérez, Valerie Lang, Elisa Garde-Lapido, Monika Gonzalez-Lopez, Orhi Barroso-Gomila, Alfred Vertegaal, et al.

▶ **To cite this version:**

Immacolata Giordano, Lucia Pirone, Veronica Muratore, Eukene Landaluze, Coralia Pérez, et al.. SALL1 modulates CBX4 stability, nuclear bodies and regulation of target genes. Frontiers in Cell and Developmental Biology, 2021, 9, pp.715868. 10.3389/fcell.2021.715868 . hal-03370040

HAL Id: hal-03370040
https://hal.science/hal-03370040v1

Submitted on 7 Oct 2021

HAL is a multi-disciplinary open access archive for the deposit and dissemination of scientific research documents, whether they are published or not. The documents may come from teaching and research institutions in France or abroad, or from public or private research centers.

L'archive ouverte pluridisciplinaire **HAL**, est destinée au dépôt et à la diffusion de documents scientifiques de niveau recherche, publiés ou non, émanant des établissements d'enseignement et de recherche français ou étrangers, des laboratoires publics ou privés.

SALL1 modulates CBX4 stability, nuclear bodies and regulation of target genes.

Immacolata Giordano[1,†], Lucia Pirone[1,#,†], Veronica Muratore[1], Eukene Landaluze[1], Coralia Pérez[1], Valerie Lang[2], Elisa Garde-Lapido[1], Monika Gonzalez-Lopez[1], Orhi Barroso-Gomila[1], Alfred C. O. Vertegaal[3], Ana M. Aransay[1,4], Jose Antonio Rodriguez[5], Manuel S. Rodriguez[6], James D Sutherland[1,*], Rosa Barrio[1,*]

1. Center for Cooperative Research in Biosciences (CIC bioGUNE), Basque Research and Technology Alliance (BRTA), Bizkaia Technology Park, Building 801A, Derio, Spain.

2. Viralgen Vector Core, Parque Científico y Tecnológico de Guipúzcoa, Paseo Mikeletegui 83, 20009 San Sebastián, Spain.

3. Cell and Chemical Biology, Leiden University Medical Center (LUMC), 2333 ZA Leiden, The Netherlands.

4. CIBERehd, Instituto de Salud Carlos III, C/ Monforte de Lemos 3-5, Pabellón 11, Planta 0, 28029 Madrid, Spain.

5. Department of Genetics, Physical Anthropology and Animal Physiology, University of the Basque Country (UPV/EHU), Leioa, Spain.

6. Laboratoire de Chimie de Coordination (LCC)-CNRS, UPS, 31400, Toulouse, France.

(*) Corresponding authors: jsutherland@cicbiogune.es, rbarrio@cicbiogune.es

R Barrio ORCID: 0000-0002-9663-0669

JD Sutherland ORCID: 0000-0003-3229-793X

(#) Present address: Council for Agricultural Research and Economics. Research Centre for Plant Protection and Certification (CREA-DC), Rome, Italy.

(†) These authors share first authorship.

Running title: CBX4 regulation by SALL1

Keywords: CBX4, SALL1, nuclear bodies, SUMO, ubiquitin

ABSTRACT

Development is orchestrated through a complex interplay of multiple transcription factors. The comprehension of this interplay will help us to understand developmental processes. Here we analyze the relationship between two key transcription factors: CBX4, a member of the Polycomb Repressive complex 1 (PRC1), and SALL1, a member of the Spalt-like family with important roles in embryogenesis and limb development. Both proteins localize to nuclear bodies and are modified by the Small Ubiquitin-like Modifier, SUMO. Our results show that CBX4 and SALL1 interact in the nucleoplasm and that increased SALL1 expression reduces ubiquitination of CBX4, enhancing its stability. This is accompanied by an increase in the number and size of CBX4-containing Polycomb bodies, and by a greater repression of CBX4 target genes. Thus, our findings uncover a new way of SALL1-mediated regulation of Polycomb bodies through modulation of CBX4 stability, with consequences in the regulation of its target genes, which could have an impact in cell differentiation and development.

INTRODUCTION

Development of higher organisms is orchestrated by a complex interplay of regulatory networks involving multiple signaling pathways and transcriptional regulatory factors. Two key families of transcriptional repressor proteins involved in development are the Polycomb Group (PcG) and the Spalt-like (SALL) proteins.

PcG proteins are involved in epigenetic regulation and control cell fate during embryonic development. These proteins accumulate in nuclear foci called Polycomb (Pc) bodies, which are involved in transcriptional repression (Saurin et al., 1998; Cheutin and Cavalli, 2012; Entrevan et al., 2016; Schuettengruber et al., 2017) and form two distinct complexes: Pc Repressive Complex1 and 2 (PRC1 and PRC2), conserved from flies to human. A crucial component of the PRC1 complex is CBX4. CBX4 is required to maintain the transcriptionally repressive state of HOX genes during development, and has an important role in several essential pathways. Thus, it has been described to facilitate differentiation of hematopoietic stem cells (Klauke et al., 2013), counteracting cellular senescence (Ren et al., 2019) and maintaining the epithelial lineage identity via repression of non-epidermal lineage and cell cycle inhibitor genes (Mardaryev et al., 2016). Moreover, CBX4 is recruited rapidly to sites of DNA damage (Ismail et al., 2012) and has emerged as a critical component of the DNA end resection machinery (Soria-Bretones et al., 2017).

SALL family members (SALL1 to SALL4), on the other hand, are important regulators of animal development, being crucial for the formation of the limbs, kidneys and the central and peripheral nervous systems, among other organs (de Celis and Barrio, 2009). SALL proteins are characterized by the presence of several precisely spaced copies of the zinc finger domain (de Celis and Barrio, 2009). They

also contain a N-terminal glutamine-rich region, which could have a role in dimerization or protein-protein interactions (Kohlhase et al., 1998; Buck et al., 2000; Sweetman et al., 2003; Borozdin et al., 2006), and a conserved N-terminal motif that mediates its interaction with one of the major corepressor complexes in mammalian cells, the Nucleosome Remodeling Deacetylase (NuRD) complex (Kiefer et al., 2002; Lauberth and Rauchman, 2006). Like the PcG proteins, SALL1 and its homologues localize in nuclear bodies, as it has been reported in cultured cells and *in vivo* (Netzer et al., 2001; Kiefer et al., 2002; Sánchez et al., 2010; Abedin et al., 2011). However, the nature and function of these bodies have not been explored.

CBX4 and SALL1 play important roles in different aspects of human health. Dysregulation of CBX4 contributes to the occurrence and progression of human tumors, in which it can act as either oncogene or tumor suppressor, depending on the cellular context (Wang et al., 2016). Mutations in *SALL1*, on the other hand cause Townes-Brocks Syndrome (TBS), an autosomal dominant syndrome characterized by renal anomalies, hearing loss, congenital heart defects, and eye anomalies among other symptoms (Kohlhase, 1993). TBS-causing mutations produce truncated SALL1 proteins lacking most of the zinc finger pairs, which aberrantly localize to the cytoplasm and interfere with centrosomal components, resulting in the formation of longer and more abundant primary cilia in patient-derived cells (Bozal-Basterra et al., 2018; Bozal-Basterra et al., 2020).

As described for many other transcriptional regulatory factors, the localization and activity of CBX4 and SALL1 can be modulated by post-translational modifications, including conjugation to ubiquitin or ubiquitin-like (UbL) proteins, such as Small Ubiquitin-like Modifier (SUMO). Thus, CBX4 is SUMOylated and it is a substrate of the SUMO-deconjugating enzyme SENP2 (Wotton and Merrill, 2007;

98 Kang et al., 2010). In addition, it was identified as a SUMO substrate in different
99 proteomic analyses (Golebiowski et al., 2009; Galisson et al., 2011; Hendriks et al.,
100 2014; Lamoliatte et al., 2014; Tammsalu et al., 2014; Hendriks et al., 2015; Xiao et
101 al., 2015; Hendriks and Vertegaal, 2016). Interestingly, CBX4 itself is proposed to be
102 a SUMO E3 ligase, and is involved in SUMOylation of the transcriptional corepressor
103 C-terminal-binding protein (CtBP) (Kagey et al., 2003), the nucleocytoplasmic
104 shuttling protein hnRNP (Pelisch et al., 2012), the transcriptional co-activator Prdm16
105 (Chen et al., 2018) and other chromatin-associated factors including CTCF, Dnmt3a
106 or Bm1 (Li et al., 2007; MacPherson et al., 2009; Ismail et al., 2012). CBX4 has also
107 been found ubiquitinated and its polyubiquitination influences the dynamics of the
108 PRC1 at the chromatin and the regulation of downstream genes (Povlsen et al., 2012;
109 Mertins et al., 2013; Udeshi et al., 2013; Ning et al., 2017; Akimov et al., 2018; Wang
110 et al., 2020).

111 In the case of SALL1, interaction with SUMO1 and the SUMO E2 conjugase
112 UBC9 has been reported using yeast two-hybrid and *in vitro* assays, with
113 SUMOylation mapped to lysine 1086 (Netzer et al., 2002). Subsequently, SALL1 as
114 well as other SALL proteins, have been confirmed as targets of SUMOylation by
115 proteomics analyses (Golebiowski et al., 2009; Galisson et al., 2011; Hendriks et al.,
116 2014; Schimmel et al., 2014; Hendriks et al., 2015; Xiao et al., 2015; Hendriks and
117 Vertegaal, 2016). In *Drosophila*, SUMOylation of SALL homologues influences their
118 role in vein pattern formation in the wing and their transcriptional repressor activity
119 (Sánchez et al., 2010; Sánchez et al., 2011).

120 Remarkably, although different functional aspects of CBX4 and SALL1 have
121 been addressed in previous studies, a regulatory interplay between these proteins has
122 not been described so far. Interestingly, we identified CBX4, as well as other PcG

proteins, as a possible interactor of SALL1 by proximity proteomics (Bozal-Basterra et al., 2018). In addition, *sall* genes and *Pc* interact genetically in *Drosophila*, as mutations in the homologue *spalt-major* enhanced the phenotypical effects of Pc group mutations during embryogenesis (Casanova, 1989; Landecker et al., 1994). These findings, together with the localization of both proteins to nuclear bodies, as well as the regulation by SUMO of both proteins, prompted us to further investigate a potential functional or regulatory interplay between SALL1 and CBX4. We report here a novel interaction between these two transcriptional regulators in the nucleoplasm. Interestingly, SALL1 influences the stability of CBX4 by modulating its ubiquitination, which might be related to changes in the regulatory capacity of CBX4 over HOX genes. Overall, we present here a novel mechanism of regulation of a crucial factor in development, which has consequences for the regulation of its target genes.

MATERIALS AND METHODS

Cell culture and cell transfection

Human U2OS (ATCC HTB-96) and HEK 293FT (Invitrogen) cells, as well as derived cell lines, were cultured at 37ºC with 5% of CO2 in DMEM (Dulbecco's modified Eagle's medium; Gibco) supplemented with 10% FBS and 1% penicillin/streptomycin (Gibco). HEK 293FT cells were transiently transfected using calcium phosphate in 10 cm dishes with 3-10 µg of DNA using different sets of plasmids according to each experiment. Briefly, DNA was mixed with 500 µl of 2.5 M $CaCl_2$ and H_2O (1:10). The was added drop by drop to the same volume of HBS

148 (NaCl 280 mM, KCl 10 mM, Na2HPO4 1.5 mM, Glucose 12 mM, HEPES 50 mM),
149 incubated for 10-15 minutes and added to the cells. U2OS cells were transiently
150 transfected using PEI (Sigma Aldrich #408727), or Effectene (Qiagen) according to
151 the manufacturers' instructions.
152
153 **Generation of plasmids**
154 The following plasmids were used in this study (Table 1). DNA fragments
155 were amplified from the indicated plasmids by high-fidelity PCR Platinum SuperFi
156 (Thermo). PCR products were purified using mi-Gel Extraction kit (Metabion),
157 digested if necessary using the restriction enzymes (Fermentas; NEB) and assembled
158 by ligation or using NEBuilder HiFi Master Mix (NEB). All resulting plasmids were
159 checked by sequencing. Cloning details are available upon request.
160
161 **Table 1. Plasmids used in the study**

Name of the vector	Reference	Parental vectors	Cloning sites/notes
CAG-bioSUMO3-T2A-BirA^{opt}-T2A-GFPpuro	(Pirone et al., 2017)	-	-
CMV-CBX4-YFP	This work	*pEYFP-N1*	*Eco*RI-*Sal*I (KAN); CBX4 generated by high-fidelity PCR
CMV-SALL1-YFP	(Pirone et al., 2017)	*pEYFP-N1*	*Eco*RI-*Sal*I (KAN); SALL1 generated by high-fidelity PCR
CMV-SALL1ΔSUMO-YFP	This work	*CMV-SALL1-YFP*	*Eco*RI-*Sal*I; mutants introduced by overlap extension PCR (KAN); K571R; K592R; K982R; K1086R
CMV-SALL1ΔSIM-YFP	This work	*CMV-SALL1-YFP*	*Eco*RI-*Sal*I; mutants introduced by overlap extension PCR (KAN); predicted SIMs mutated to AAAA;

			SIM71: VLIV; SIM195: VIIE; SIM254: ILLL; SIM1252: ISVI
CMV-SALL1-2xHA	This work	*CMV-SALL1-YFP*	EYFP exchanged for 2xHA using *Sal*I-*Not*I (KAN)
CMV-SALL1^{826}-2xHA	This work	*CMV-SALL1(826)-YFP*	EYFP exchanged for 2xHA using *Sal*I-*Not*I (KAN)
CB6-HA-N	M. Way lab (CRUK, London)	*CB6*	CB6 has CMV promoter and confers neo selection; contains N-terminal HA epitope and MCS (AMP)
CMV-EGFP-β-galactosidase	This work	*pEGFP-N1*	LacZ subcloned from pIND/lacZ (Invitrogen)
CB6-HA-SALL1	This work	*CB6-HA-N*	*SALL1* from *CMV-SALL1-YFP*
CB6-HA-SALL1ΔSUMO	This work	*CB6-HA-N*	*SALL1* from *CMV-SALL1 ΔSUMO-YFP*
CB6-HA-CBX4	This work	*CB6-HA-N*	CBX4 from *CMV-CBX4-YFP*
*CMV-SALL1-BirA**	This work	*CMV-SALL1-YFP*	*Exchanged YFP for BirA*(BioID) by Sal1-Not1*
*CMV-Pc-BirA**	This work	*CMV-SALL1-BirA**	*Drosophila Pc* (PCR amplified) exchanged for SALL1 using *Eco*R1-*Sal*1 (KAN); Pc source: Addgene #1927
*CMV-CBX4-BirA**	This work	*CMV-SALL1-BirA**	*CBX4* (PCR amplified) exchanged for *SALL1* using *Eco*R1-*Sal*1 (KAN)
CMV-BirAopt-2A-puro	(Pirone et al., 2017)	-	-
CMV-bioUB-2A-BirAopt-2A-puro	(Pirone et al., 2017)	-	-
LL-CMV-GFS-SALL1-IRES-puro	This work	LL-CMV-GFS-IRES-puro	SALL1 inserted into modified version of Lentilox3.7; expresses N-terminal GFP-FLAG-STREP

			tag
TripZ-SALL1-2xHA-puro	This work	*CMV-SALL1-2xHA; TRIPZ*	Inserted SALL1-2xHA amplicon into BshT1-Mlu1TRIPZ (Dharmacon)
pcDNA3	Invitrogen	-	-
Lenti-Cas9-blast vector	Addgene #52962	-	-
psPAX2	Addgene #12260	-	-
pMD2.G (VSV-G envelope)	Addgene #12259	-	-
pEYFP-N1, pEYFP-C	Clontech	-	-

(KAN) or (AMP) indicate the antibiotic resistant cassette (kanamycin or ampicillin, respectively) in the vector for bacterial transformation.

Lentiviral transduction

Lentiviral expression constructs were packaged using psPAX2 and pMD2.G in HEK 293FT cells, and cell culture supernatants were used to transduce HEK 293FT cells to generate stable cell populations expressing SALL1 (constitutive: LL-GFS-SALL1-IRES-puro; or inducible: TripZ-SALL1-2xHA-puro). Selection was performed using 1 µg/ml of puromycin.

Bioinformatics analyses

SUMOylation sites and SUMO-interacting motif predictions were searched using SUMOplot (http://www.abgent.com/sumoplot), GPS-SUMO (http://sumosp.biocuckoo.org; (Zhao et al., 2014)), and JASSA programs (Beauclair et al., 2015). Sequence search and comparison was performed using BLAST (http://blast.ncbi.nlm.nih.gov/Blast.cgi/). Alignments were performed using Clustal (https://www.ebi.ac.uk/Tools/msa/clustalo/).

SUMOylation and Ubiquitination assays in cultured cells

For the isolation of SUMOylated SALL1, one 10 cm dish of HEK 293FT cells was transfected with 7 µg of *CMV-SALL1-2xHA, CMV-SALL1ΔSUMO-2xHA,* and 3µg of *CAG-bioSUMO3-T2A-BirA^{opt}-T2A-GFPpuro* or *CAG-BirA^{opt}-T2A-GFPpuro* as control. Isolation of SUMOylated protein was done according to previously reported methodology (Pirone et al., 2016; Pirone et al., 2017).

For the ubiquitination assay of CBX4, one 10 cm dish was transfected with 5 µg of *CMV-SALL1-YFP*, *CMV-SALL1ΔSUMO-YFP*, *CMV-GFP-β-Galactosidase*, *CMV-BirA-2A-puro*, *CMV-bioUB-2A-BirA-2A-puro*, or *CB6-HA-CBX4*. After transfection, medium was supplemented with biotin at 50 µM. 24 hours after transfection, plates were treated with MG132 (10 µM, 12 hours; Calbiochem). Transfected cells were collected after 48–72 hours, washed 3 times with phosphate buffered saline (PBS) and resuspended in lysis buffer [0.5 ml/10 cm dish; 8 M urea, 1% SDS, 50 mM N-ethylmaleimide, 1x protease inhibitor cocktail (Roche) in 1x PBS]. Sonication was performed to reduce sample viscosity and samples were cleared by centrifugation at room temperature (RT). High-capacity NeutrAvidin-agarose beads (Thermo Scientific) were equilibrated and 30-60 µl suspension was used for incubation with extracts (12-18 hours; RT; gentle agitation). Beads were subjected to stringent washes using the following washing buffers all prepared in 1x PBS (Franco et al., 2011): WB1 (8 M urea, 0.25% SDS); WB2 (6 M Guanidine-HCl); WB3 (6.4 M urea, 1 M NaCl, 0.2% SDS), WB4 (4 M urea, 1 M NaCl, 10% isopropanol, 10% ethanol and 0.2% SDS); WB5 (8 M urea, 1% SDS); and WB6 (2% SDS). Samples were eluted in 50 µl of Elution Buffer (4x Laemmli sample buffer, 100 mM DTT) by two cycles of heating (5 minutes; 99 °C), with vortexing in between. Beads were separated by centrifugation (18000x g, 5 minutes).

For the isolation of ubiquitinated endogenous CBX4 from cells lysates, 10 cm dishes were transfected with 5 µg of *CMV-SALL1-2xHA* plasmid or with with pcDNA3 plasmid as control. After 48 hours, cells were washed three times with 1x PBS and lysed in 500 µl of TUBEs buffer [20 mM Phosphate buffer, pH 7.5 (Sigma), 2 mM EDTA (Sigma), 50 mM sodium fluoride (Sigma), 5 mM tetra-sodium pyro-phosphate (Sigma), and 10 mM β-glycerol 2-phosphate (Sigma)]. The buffer was filtered through a 0.22 µm membrane and stored at 4°C. 80 µl of the lysate were taken as input. Ubiquitinated material was isolated using Tandem Ubiquitin Binding Entities (TUBEs) based on RAD23 Homolog A (RAD23A) ubiquitin binding domains fused to GST and expressed in bacteria (Hjerpe et al., 2009; Aillet et al., 2012). To eliminate proteins with binding affinity for the beads (Glutathione Sepharose 4B, GE Healthcare), lysates were incubated with 125 µg of GST bound to glutathione-agarose beads for 1 hour at 4°C and centrifugated for 2 minutes at 1000 rpm. After washing GST-TUBES beads with cold 1x PBS twice, supernatants were added, incubated for 1 hour at 4°C and centrifugated for 2 minutes at 1000 rpm. The supernatants were then removed and beads were washed 3 times with TUBEs buffer. The beads were washed 3 times with PBS-Tween 0.5% and twice with TUBEs buffer containing NaCl (0.5 M). Finally, the beads were resuspended in 50 µl of Boiling buffer (50 mM Tris–HCl pH 6.8, 10% glycerol, 2% SDS, Bromophenol Blue, 10% β-mercaptoethanol) warmed at 60°C before use.

In vitro SUMOylation

Using PCR templates with incorporated 5' T7 priming site +/- 3' epitope-tags, SALL1-2xHA and CBX4 were transcribed/translated *in vitro* using the TNT ® Quick Coupled Transcription/Translation System (Promega) according to the manufacturer's

instruction and were then incubated in a buffer containing an ATP regenerating system [(50 mM Tris pH 7.5, 10 mM MgCl2, 2 mM ATP, 10 mM creatine phosphate (Sigma), 3.5 U/ml of creatine kinase (Sigma), and 0.6 U/ml of inorganic pyrophosphatase (Sigma)], 10 µg of SUMO1 or a combination of 5 µg of SUMO2 and SUMO3, 0.325 µg UBC9 and 0.8 µg of purified SAE1/2 (ENZO Life Sciences). SALL1 SUMOylation was checked adding 0.5 to 2 µl of *in vitro* transcribed/translated protein in the SUMOylation assay. Reactions were incubated at 30°C for 2 hours and stopped by addition of SDS sample buffer.

GFP-Trap co-pulldown

HEK 293FT cells were plated at 25-30% confluence. Transient transfections were performed using calcium phosphate in a 10 cm dish with 5 µg of *CMV-CBX4-YFP, CMV-SALL1-YFP, CMV-SALL1ΔSUMO-YFP, CMV-SALL1ΔSIM-YFP, CMV-YFP, CMV-SALL1-2xHA, CMV-SALL1-826-2xHA, CB6-HA, CB6-HA-SALL1, CB6-HA-SALL1ΔSUMO* or *CB6-HA-CBX4* in complete medium. All steps after transfection were performed at 4°C. Two days after transfection, cells were washed 3 times with cold 1x PBS and detached from the dish with a scraper. Cells of 10 cm dishes were lysed by adding 1 ml of Lysis Buffer [25 mM Tris-HCl pH 7.5, 150 mM NaCl, 1 mM EDTA, 1% NP-40, 0.5% Triton X-100, 5% glycerol, protease inhibitors (Roche)] followed by incubation on a rotating wheel for 30 minutes at 4°C. Lysates were sonicated and spun down at 25000x g for 20 minutes. After saving 40 µl of supernatant (input), the rest of the lysate was incubated overnight with 30 µl of equilibrated GFP-Trap resin (Chromotek) in a rotating wheel. Beads were washed 5 times for 5 minutes each with washing buffer (25 mM Tris-HCl pH 7.5, 300 mM NaCl, 1 mM EDTA, 1% NP-40, 0.5% Triton X-100, 5% glycerol). Beads were

centrifuged at 2000x g for 2 minutes after each wash. For elution, samples were boiled for 5 minutes at 95°C in 2x Laemmli buffer.

BioID analysis of interactions

Proximity interaction between CBX4 or Pc proteins to SALL1 was verified by the BioID method (Roux et al., 2013), consistent on fusing them to a promiscuous form of the enzyme BirA (BirA*) and to isolate the biotinylated material by streptavidin-beads pulldowns. HEK 293FT cells were transfected with 5 µg of CMV-CBX4-BirA* or CMV-Pc-BirA* in combination with *CMV-SALL1-2xHA* or *CMV-SALL1826-2xHA*. After 24 hours, the medium was supplemented with 50 mM of biotin. At 48 hours, cells were washed three times in cold 1x PBS and collected in 1 ml of lysis buffer [8 M urea, 1% SDS, protease inhibitor cocktail (Roche) in 1x PBS]. Lysates were sonicated and cleared by centrifugation, incubated overnight with 40 µl of equilibrated NeutrAvidin-agarose beads (Thermo Scientific) and washed with WB1 to 6 as indicated in the ubiquitination protocol above. Elution was done as previously described using 50 µl of Elution Buffer (4x Laemmli sample buffer, 100 mM DTT) by two cycles of heating (5 minutes, 99 °C), with vortexing in between. Beads were separated by centrifugation (18000x g, 5 minutes).

Cycloheximide assay

3 x 10^5 HEK 293FT cells per well were plated in 6-well plates. Four hours later, cells were transfected with 2 µg of *CMV-SALL1-YFP, CMV-SALL1ΔSUMO-YFP* or *CMV-GFP-β-Galactosidase* plasmid per well using the calcium phosphate method. 24 hours after transfection, cells were treated with 50 µg of cycloheximide (CHX, 50 µg/ml) in combination or not with MG132 (10 µM) for different time points (0, 4, 8

or 16 hours). Cells were lysed in RIPA buffer [150 mM NaCl, 1.0% NP-40, 0.5% sodium deoxycholate, 0.1% SDS, 50 mM Tris, pH 8.0, protease inhibitors (Roche)] and analyzed by Western blot.

Western blot

Samples were boiled at 95° for 5 minutes. Proteins were separated by SDS-PAGE (BioRad) and blotted using wet transfer to nitrocellulose membranes (0.45 μm pore; Cytiva). Membranes were blocked in 1x PBS with 0.1% Tween-20 (PBS-T) and 5% non-fat dry milk (blocking buffer) for 1 hour and, for biotin detection, Casein Blocking Buffer 1x (Sigma #B6429). After that, membranes were incubated in blocking buffer for 1 hour at RT or overnight at 4°C with the following primary antibodies: mouse monoclonal anti-HA (Sigma, 1:1000, #H3663), mouse monoclonal anti-β-Actin (Sigma, 1:1000, #A2228), mouse monoclonal anti-GFP (Roche, 1:1000, #11814460001), mouse monoclonal anti-SALL1 (R&D, 1:1000, #PP-K9814-00), rabbit polyclonal anti-CBX4 (Proteintech, 1:1000, #18544-1-AP), rabbit polyclonal anti-Avitag (GeneScript, 1:1000, #A00674), or rabbit monoclonal Vinculin (Cell Signaling, 1:1000, #13901S).

After three washes with PBS-T, the blots were incubated for 1 hour with secondary antibodies: HRP-conjugated anti-mouse or anti-rabbit (1:5000, Jackson ImmunoResearch # 115-035-062 or # 111-035-045, respectively), HRP-conjugated anti-biotin (1:1000, Cell Signaling Technology #7075), HRP-conjugated anti-tubulin (1:5000, Proteintech #66031), or HRP-conjugated anti-GAPDH (1:5000, Proteintech #60004). Membranes were washed three times in PBS-T, developed using Clarity Western ECL substrate (Biorad) or Super Signal West Femto (Pierce), and chemiluminescent signals detected using a ChemiDoc camera system (Biorad).

Quantification of bands was performed using Fiji software and normalized to Actin, GAPDH or Vinculin levels, unless otherwise indicated. At least three independent blots were quantified per experiment.

Immunostaining and microscopy analysis

For immunostaining and microscopy analysis, 50000 cells per well were seeded in a 24 well-plate on 12 mm diameter round acid-washed sterile coverslips. U2OS cells were transfected with 2 µg of *CMV-SALL1-YFP, CMV- SALL1ΔSUMO-YFP* or *pEYFP-C1,* 1.5 µg of *CMV-SALL1-YFP* or HEK 293FT_TripZ-SALL1-2xHA were used.

After 2 days cells were washed 3 times with cold 1x PBS, fixed in 4% paraformaldehyde (Santa Cruz) supplemented with 0.1% Triton X-100 in 1x PBS for 20 minutes at RT. Then, coverslips were washed 3 times with 1x PBS to remove the fixative. Blocking was performed in blocking buffer (1% BSA, 0.3% Triton X-100, 25 mM NaCl in 1x PBS) for 1 hour at RT. Incubation with primary antibodies diluted in blocking solution was performed during 1 h at 37°C in a humidity chamber or overnight at 4°C. The following primary antibodies were used: rabbit polyclonal anti-SALL1 (1:200, Abcam #31905), mouse monoclonal anti-GFP (1:500, Roche #11814460001), mouse monoclonal anti-PML (Promyelocytic Leukemia Protein) (1:100, Santacruz #sc-966), mouse monoclonal anti-SC35 (Splicing Component, 35 KDa, also known as Serine And Arginine Rich Splicing Factor 2) (1:200. BD Pharmingen #556363), rabbit polyclonal anti-CBX4 (1:100, Proteintech #18544-1-AP), rabbit polyclonal anti-SUMO2/3 (1:100, Eurogentec #AV-SM23-0100), mouse monoclonal anti SUMO1 (1:100, Developmental Studies Hybridoma Bank, DSHB, #21C7) or mouse monoclonal anti-SUMO2 (1:100, DSHB #8A2). Endogenous

SALL1 or SALL1-2xHA in HEK 293FT_TripZ-SALL1-2xHA cells were stained by a primary antibody against SALL1 (R&D, 1:100, #PP-K9814-00).

After incubation with the primary antibody, cells were gently washed 3 times with 1x PBS and then incubated with the secondary antibody in the dark for 1 hour at RT. The secondary antibodies conjugated to fluorophores used were donkey anti-mouse or anti-rabbit Alexa Fluor 488, Alexa Fluor 568 or Alexa Fluor 647 (1:200, Molecular Probes). To visualize the nuclei, we incubated the cells with DAPI (1:15000, Roche #10236276001) for 5 minutes at RT. Another 3 washes were performed to remove unbound secondary antibody. Finally, coverslips were mounted using Prolong Gold antifade reagent (Molecular Probes #P36930) and stored in the dark at 4°C.

Stained cells were visualized using an Upright Fluorescent Microscope Axioimager D1 or a Leica SP2 or SP8 confocal microscope with 63x objective. For the quantification of Pc bodies, Fiji software was used.

Proximity Ligation Assays

U2OS cells were plated and transfected by PEI in 6-well plates with 2 µg of *CMV-SALL1-2xHA* or *pcDNA3*. After 2 days, cells were transferred to an 8-well chamber slide (LabTek #177410) and allowed to attach for 12 hours. Proximity Ligation Assay (PLA) was performed using the Duolink In Situ Red kit (Olink Biosciences; (Gullberg et al., 2004; Söderberg et al., 2006) according to the manufacturer's instructions. Primary antibodies used: mouse monoclonal anti-SALL1 (1:250, R&D Systems #PP-K9814-00); rabbit polyclonal anti CBX4 (1:100, Proteintech #18544-1-AP). Images were recorded on a Leica SP8 confocal microscope system using 488 nm and 561 nm wavelengths for excitation and a 63x

lens for magnification, and were analyzed with the Leica confocal software, Adobe Photoshop and ImageJ softwares.

Reverse transcription-quantitative PCR (RT-qPCR) analysis

HEK 293FT cells transfected with 5 µg of *CMV-SALL1-YPF, CMV-SALL1ΔSUMO-YFP* or *CMV-GFP-β-Galactosidase* plasmids, or HEK 293-TripZ-SALL1-2xHA_puro cells induced with different concentrations of doxycycline (dox), were used for RT-qPCR analysis. 48 hours after transfection, or 72 hours after induction, total RNA was obtained by using EZNA Total RNA Kit (Omega) and quantified using a Nanodrop spectrophotometry. cDNAs were prepared using the SuperScript III First-Strand Synthesis System (Invitrogen) using 1 µg of total RNA in 20 µl volume per reaction. qPCR was done using PerfeCTa SYBR Green SuperMix Low Rox (Quantabio). Reactions were performed in 20 µl, adding 5 µl of cDNA and 0.5 µl of each primer (10 µM), in a CFX96 thermocycler (BioRad) using the following protocol: 95ºC for 5 minutes and 40 cycles of 95ºC for 15 seconds, 56ºC or 62ºC for 30 seconds and 72ºC 20 seconds. Melting curve analysis was performed for each pair of primers between 65ºC and 95ºC, with 0.5ºC temperature increments every 5 seconds. Relative gene expression data were analyzed using the ΔΔCt method (Livak and Schmittgen, 2001). Reactions were carried out in duplicate and results were derived from at least three independent experiments, normalized to GAPDH and presented as relative expression levels. Primer sequences are listed in Table 2.

Table 2. Oligonucleotide sequences used for RT-qPCR.

Name	Sequence
hHoxa11_for	5'-AACGGGAGTTCTTCTTCAGCGTCT-3´
hHoxa11_rev	5'-ACTTGACGATCAGTGAGGTTGAGC-3´
hHoxb4_for	5'-AGGTCTTGGAGCTGGAGAAGGAAT-3´
hHoxb4_rev	5'-GGTGTTGGGCAACTTGTGGTCTTT-3´

hHoxb7_for	5’-AGACCCTGGAGCTGGAGAAAGAAT-3´
hHoxb7_rev	5’-ATGCGCCGGTTCTGAAACCAAATC-3´
hHoxb13_for	5’-TACGCTGATGCCTGCTGTCAACTA-3´
hHoxb13_rev	5’-AGTACCCGCCTCCAAAGTAACCAT-3´
hHoxc6_for	5’-AGGACCAGAAAGCCAGTATCCAGA-3´
hHoxc6_rev	5’-ATTCCTTCTCCAGTTCCAGGGTCT-3´
hHoxc10_for	5’-TGAAATCAAGACGGAGCAGAGCCT-3´
hHoxc10_rev	5’-TTGCTGTCAGCCAATTTCCTGTGG-3´
hHoxc12_for	5’-AGGGAACTCTCAGACCGCTTGAAT-3´
hHoxc12_rev	5’-AGAGCTTGCTCCCTCAACAGAAGT-3´
hHoxd13_for	5’-ATGTGGCTCTAAATCAGCCGGACA-3´
hHoxd13_rev	5’-AGATAGGTTCGTAGCAGCCGAGAT-3´
hGata4_for	5’-TCTCAGAAGGCAGAGAGTGTGTCA-3´
hGata4_rev	5’-GGTTGATGCCGTTCATCTTGTGGT-3´
hGAPDH_for	5’-CATGTTCGTCATGGGTGTGAACCA-3´
hGAPDH_rev	5’-AGTGATGGCATGGACTGTGGTCAT-3´
hSALL1_for	5’-GCTTGCACTATTTGTGGAAGAGC -3’
hSALL1_rev	5’-GAACTTGACGGGATTGCCTCCT-3`
hCBX4_for	5`-CATCGAGAAGAAGCGGATCCGCAAG-3`
hCBX4_rev	5`-CTGTTCTGGAAGGCGATCAGCAGCC-3’

Statistical analysis

Statistical analysis was performed using GraphPad 7.0 software. Data were analyzed by Shapiro-Wilk normality test and Levene´s test of variance. We used Mann Whitney-U test or Unpaired T-test for comparing two groups and One-way ANOVA for more than two groups. P values were represented by asterisks as follows: (*) P-value < 0.05; (**) P-value < 0.01; (***) P-value < 0.001; (****) P-value < 0.0001. Differences were considered significant when $P < 0.05$.

RESULTS

SALL1 does not colocalize with CBX4 in nuclear bodies

In agreement with previous reports (Netzer et al., 2001; Kiefer et al., 2002; Sánchez et al., 2010; Abedin et al., 2011), we detected endogenous SALL1 in discrete domains in the nucleus of U2OS human osteosarcoma cells (Figure S1A). Similar results were obtained in U2OS cells transfected with human SALL1-YFP (Figure S1B, C). These SALL1 foci were reminiscent of Pc bodies, where PRC proteins, such as CBX4 accumulate. Thus, we hypothesized that SALL1 and CBX4 could colocalize in nuclear bodies.

To test this hypothesis, *SALL1-YFP* plasmid was transfected into U2OS cells, where endogenous CBX4 was visualized by immunofluorescence using anti-CBX4 specific antibodies. However, SALL1 and CBX4 were found to localize to different subsets of nuclear bodies (Figure 1A).

In order to further characterize the nature of CBX4 and SALL1 bodies, we explored their possible colocalization with SUMO. We transfected U2OS cells with SALL1-YFP and examined its localization, and that of endogenous CBX4, with SUMO using immunofluorescence. While CBX4 did not colocalize with SUMO1 or SUMO2/3 (Supplementary Figure S2A, B), a partial colocalization between SALL1 and SUMO proteins was observed: some of the SALL1 bodies clearly colocalized with SUMO1 and SUMO2/3, while other SALL1 bodies did not (Figure 1 and Supplementary Figure S2E). Conversely, some SUMO1 and SUMO2/3 bodies colocalized with SALL1, while others did not. These results fit with the well-known heterogenic nature of nuclear bodies (Zidovska, 2020). Neither CBX4, nor SALL1 colocalize with other nuclear factors, such as PML (Supplementary Figure S2C, H) or SC35 (Supplementary Figure S2D, I)

As shown previously, SALL1 undergoes SUMOylation in cells (Pirone et al., 2017), which might modulate its localization. To test this possibility, we generated a SALL1 SUMO mutant (SALL1ΔSUMO) by mutating four lysine residues (K571, K592, K982 and K1086) to arginine (Supplementary Figure S3A). These residues correspond to the four SUMOylation motifs conserved in vertebrates, predicted by SUMOplot and GPS-SUMO programs with highest scores (Supplementary Figure S3C, S3D) and the motif IKED (K982) being previously identified by proteomic analysis (Xiao et al., 2015; Hendriks and Vertegaal, 2016). As predicted, the SALL1ΔSUMO mutant lost the capacity to be SUMOylated in cells (Supplementary Figure S3B). Therefore, we considered SALL1ΔSUMO a SUMO-deficient mutant of SALL1. Interestingly, neither the lack of colocalization with CBX4, nor the partial colocalization with endogenous SUMO1 and SUMO2/3 were visibly altered when SALL1ΔSUMO-YFP was analyzed (Figure 1B, E and Supplementary Figure S2F). These results, indicating that the localization of SALL1 to a subset of SUMO bodies does not depend on its SUMOylation status, raised the possibility that SALL1 localization to these foci might be mediated by the presence of SUMO-interacting motifs (SIMs) in this protein.

By analyzing the amino acid sequence of SALL1, we noted the presence of four high-scored SIMs (Supplementary Figure S3A, D). To investigate the role of these putative SIMs, we generated a SALL1ΔSIM version in which the four motifs were mutated to alanines. Remarkably, localization of SALL1 was unaffected by these mutations. Thus, SALL1ΔSIM-YFP readily localized to nuclear bodies, and partially colocalized with SUMO1 and SUMO2/3, but not with CBX4 (Figure 1C, F, and Supplementary Figure S2G). The lack of colocalization between these two proteins in

nuclear bodies prompted us to re-examine the interaction results obtained previously by mass spectrometry (MS).

SALL1 interacts with CBX4 in a SUMOylation-independent manner

Previous MS results suggested that CBX4 could interact with full length SALL1 (Bozal-Basterra et al., 2018). We checked whether we could detect the CBX4-SALL1 interaction using CBX4-BioID. HEK 293FT cells were transfected with CBX4 fused to a promiscuous variant of the BirA biotin ligase (CBX4-BirA*) together with either full length SALL1-2xHA or the truncated form of SALL1^{826}-2xHA, causative of TBS. After pulldown using NeutrAvidin beads, the eluates were analyzed by Western blot. As shown in Figure 2A, CBX4 was in close proximity to both the full length and the truncated SALL1 forms (elution panel, lanes 1 and 2). *Drosophila* Pc (DmPc-BirA, the fly CBX4 homologue; lane 3) is also able to interact with full-length SALL1-HA.

We further confirmed the interaction between SALL1 and CBX4 by using pulldown experiments. CBX4-YFP was transiently overexpressed in HEK 293FT together with SALL1-2xHA or SALL1^{826}-2xHA, and GFP-Trap-based pulldown assays were carried out. SALL1-YFP was used as a positive control, since it is known to bind to the truncated mutant. As shown in Figure 2B, CBX4-YFP interacted both with full length and truncated SALL1 (elution panel, lanes 1 and 2).

SALL1 post-translational modifications could affect its interaction with other proteins. In this regard, SALL1 SUMOylation might be particularly relevant for its interaction with CBX4, which contain SIM domains (Merrill et al., 2010). In order to test whether SUMOylation could have a role in SALL1 binding to CBX4, we analyzed the SALL1ΔSUMO capability to interact with CBX4 (Figure 2C). WT

SALL1-YFP and SALL1ΔSUMO-YFP were transiently transfected in HEK 293FT cells together with CBX4-HA (lanes 4 and 5, respectively). A GFP-Trap pulldown was performed and analyzed by Western blot. Our results show that the SUMOylation-deficient SALL1 mutant was still able to interact with CBX4 (elution panel, compare lanes 4 and 5). No appreciable differences were noted between WT SALL1 and SALL1ΔSUMO in their ability to interact with CBX4.

On the other hand, since CBX4 is known to be SUMOylated *in vitro* (Kagey et al., 2003; Merrill et al., 2010), we tested whether the predicted SIMs in SALL1 could have a role in its interaction with CBX4. As shown in Figure 2C (elution panel, compare lanes 4 and 6) SALL1 WT and SALL1ΔSIM showed similar capacity to bind CBX4. While differences in the intensity of CBX4 signals between SALL1 WT, SALL1ΔSUMO and SALL1ΔSIM can be observed, these differences were mostly due to the expression levels of the YFP-tagged SALL1 proteins. For example, the higher expression levels of SALL1ΔSUMO compared to SALL1 WT are most likely directly related to the higher levels of CBX4-HA detected in the pulldown.

In summary, these results confirm SALL1/CBX4 interaction, and show that neither SALL1 SUMOylation, nor its predicted SIM motifs are necessary for binding to CBX4 in our experimental setting.

SALL1 and CBX4 interact in the nucleoplasm

Both proteins localize to the nucleus, with non-overlapping enrichment in nuclear bodies, so we thought that the SALL1-CBX4 interaction might occur in the nucleoplasm where weaker immunofluorescence signals can be observed (Supplementary Figure S4). In order to explore this possibility, we decided to apply

the Proximity Ligation Assay (PLA), a technique that allows the detection of protein-protein interactions *in situ*.

U2OS cells were transfected with *CMV-SALL1-2xHA* or with an empty *pcDNA3* vector as negative control, and anti-SALL1 and anti-CBX4 antibodies were used to perform PLA (Figure 3A-E) (Söderberg et al., 2006; Matic et al., 2010). The signal from each detected pair of PLA probes is visualized as a fluorescent spot. Our analysis of the number of spots revealed an interaction between SALL1 and CBX4 in the nucleus (Figure 3A, E). Combined with the SALL1/CBX4 localization analyses described above, these results suggest that the interaction between SALL1 and CBX4 takes place most probably in the nucleoplasm instead of in nuclear bodies.

SALL1 post-transcriptionally increases the levels of CBX4

Considering previous evidence that SALL1 can be SUMOylated and that CBX4 can act as an E3 ligase to increase SUMOylation of several substrates (Kagey et al., 2003; Li et al., 2007; MacPherson et al., 2009; Ismail et al., 2012; Pelisch et al., 2012; Chen et al., 2018), we hypothesized that the SALL1/CBX4 interaction could drive SALL1 SUMOylation. However, our *in vitro* SUMOylation assays in the presence of SUMO1 or SUMO2/3 showed that the SUMOylated form of SALL1 did not vary in a statistically significant manner when different amounts of CBX4 were added to the reaction (Supplementary Figure S5).

These results suggested that CBX4 does not function as a SUMO E3 ligase for SALL1 in this experimental settings, leaving the question of what could be the biological outcome of the interaction between these proteins unanswered. Intriguingly, while performing the experiments to validate the SALL1-CBX4 interaction, we had noticed that the levels of CBX4 were higher in cells co-transfected

512 with SALL1 proteins (SALL1 WT, SALL1ΔSUMO or SALL1ΔSIM) than in control
513 cells co-expressing YFP (Figure 2B, lanes 1 vs 5; Figure 2C, lanes 4, 5, and 6 vs 8
514 and 9). This observation was supported by a quantitative analysis of the immunoblot
515 results (Figure 2D), and was further confirmed using a transient co-expression
516 experiment in HEK 293FT cells. In this experiment, Western blot analysis revealed
517 higher levels of CBX4-HA in cells co-expressing SALL1-YFP than in cells co-
518 expressing YFP alone (Figure 4A).

519 In order to discard any potential artefact due to the transient overexpression
520 conditions, we generated two HEK 293FT-derived cell lines stably expressing
521 SALL1. On one hand, we generated a HEK 293FT cell line constitutively expressing
522 a GFS (GFP-Flag-Strep)-tagged version of SALL1 at levels moderately increased
523 over the endogenous SALL1. Western blot analysis showed increased levels of
524 endogenous CBX4 in HEK 293FT_GFS-SALL1 cells compared with parental HEK
525 293FT cells (Figure 4B). On the other hand, we used the inducible lentiviral vector
526 TripZ to generate the HEK 293FT_TripZ-SALL1-2xHA cell line (see Materials and
527 Methods). This vector, based on the Tet-On system, allowed us to induce the
528 expression of SALL1-2xHA in a doxycycline dependent manner, while preserving the
529 expression of endogenous SALL1. As verified by immunofluorescence analysis
530 (Figure 4C), increasing concentrations of doxycycline (1 ng/ml, 10 ng/ml, 0. 1 µg/ml
531 or 1 µg/ml), lead to a progressive increment of the SALL1 expression in HEK
532 293FT_TripZ-SALL1-2xHA cells. The levels of endogenous CBX4 protein were
533 analyzed in these cells using Western blot (Figure 4D, E). Quantification of three
534 independent experiments showed that CBX4 levels were significantly increased when
535 the cells were treated with 1 µg/ml of doxycycline compared to untreated cells
536 (Figure 4E).

Since SALL1 is a transcription factor, we wondered whether the increased CBX4 levels described above could be due to SALL1-mediated transcriptional activation of CBX4 expression, potentially in an indirect way, as SALL1 is mostly described as a transcriptional repressor. We tested this possibility using the inducible HEK 293FT_TripZ-SALL1-2xHA cell model. SALL1 and CBX4 mRNA expression was analyzed by RT-qPCR) in control or doxycycline-treated cells. As expected, SALL1 mRNA expression increased in a doxycycline-dependent manner (Figure 4F). However, CBX4 mRNA expression levels did not vary significantly.

Altogether these results demonstrate that increasing levels of SALL1 are correlated with increasing CBX4 protein levels and, importantly, that this effect occurs at a post-transcriptional level.

SALL1 stabilizes CBX4 avoiding its degradation via the proteasome

Different mechanisms may contribute to increase the levels of a given protein, including changes in subcellular localization, solubility, or alteration in protein stability due to reduced degradation. The results described above led us to test the hypothesis that SALL1 could stabilize CBX4.

To this end, we analyzed the half-life of CBX4 by using a time-course experiment with CHX. HEK 293FT cells were transfected with WT SALL1-YFP, SALL1ΔSUMO-YFP or GFP-β-Gal and treated with 50 μg/ml of CHX in presence or absence of 10 μM of the proteasome inhibitor MG132. Cells were collected at different time points (0, 4, 8 and 16 hours after initiation of treatment) and the levels of endogenous CBX4 were analyzed by Western blot.

As shown Figure 5A, the levels of CBX4 began to decrease after 4 h of CHX treatment in cells expressing GFP-β-Gal. However, in SALL1 WT or

SALL1ΔSUMO-transfected cells the reduction in CBX4 levels was slower than in control cells. Quantification of six independent experiments is shown in Figure 5B. When cells were co-treated with CHX and MG132 (Figure 5C), proteasome degradation was inhibited and CBX4 levels did not decline at 4 h. Consequently, as shown in the Western blot quantification, no significant differences in the CBX4 levels were observed between cells transfected with SALL1, SALL1ΔSUMO or control (Figure 5D). Overall, these results show that CBX4 protein is more stable in presence of SALL1 or SALL1ΔSUMO, and that degradation of CBX4 occurs through the ubiquitin proteasome system (UPS). Therefore, we concluded that SALL1 stabilizes CBX4 protein slowing down its degradation via the proteasome, and that SUMOylation of SALL1 seems not to be essential for CBX4 stabilization.

SALL1 influences CBX4 ubiquitination

Previous reports have shown that CBX4 is ubiquitinated to mediate its degradation through the proteasome (Ning et al., 2017). To investigate a potential relationship between SALL1 expression and CBX4 ubiquitination, we used the bioUb system (Pirone et al., 2017). First, we tested the efficiency of this system to detect the ubiquitinated fraction of CBX4. We transiently transfected HEK 293FT cells with CBX4-HA together with BirA-2A-bioUb or BirA as control. Cells were treated with biotin in presence or absence of the proteasome inhibitor MG132. Protein lysates were processed for bioUb assay (see Materials and Methods) and results were analyzed by Western blot (Figure 6A). Ubiquitinated CBX4 is shown in the elution panel. A band above 100 KDa and a high molecular weight smear, both consistent with ubiquitinated forms of CBX4, are visible. As expected, the levels of ubiquitinated CBX4 increased in presence of the proteasome inhibitor MG132. Anti-

587 Avitag antibodies detecting bioUb also showed an increase in the general
588 ubiquitination levels in presence of MG132, as shown in the elution panel. These
589 results confirmed the modification of CBX4 by ubiquitination and its degradation via
590 UPS.

591 Next, to test whether SALL1 could increase CBX4 stability by impairing its
592 ubiquitination and subsequent proteasomal degradation, we studied CBX4
593 ubiquitination in the inducible HEK 293FT_TripZ-SALL1-2xHA cells. These cells
594 were transiently transfected with *CBX4-YFP* together with *BirA-2A-bioUb* or *BirA* as
595 control. The cells were treated or not with 1 μg/ml of doxycycline to induce SALL1
596 expression, in the presence or absence of 10 μM MG132. Protein lysates were
597 processed for bioUb assay, and the results were analyzed by Western blot (Figure
598 6B). A statistically significant reduction of CBX4 ubiquitination was observed in
599 presence of high levels of SALL1 (Figure 6B, C, in the elution panel compare lane 4
600 with lane 2). However, in the presence of MG132, no significant differences were
601 appreciated between induced and not induced cells (Figure 6C, in the elution panel
602 compare lanes 6 and 8).

603 To further analyze the ubiquitination of endogenous CBX4, we transiently
604 expressed SALL1-2xHA or pcDNA3 as a control in HEK 293FT cells. After lysis,
605 total ubiquitinated material was isolated from the cells by pulldown using TUBES
606 (see Materials and Methods), and analyzed by Western blot (Figure 6D, E). In
607 presence of SALL1, the levels of ubiquitinated CBX4 were reduced when compared
608 with cells transfected with the control plasmid (elution panel, compare lanes 1 and 2).
609 No significant differences were appreciated when cells were treated with MG132
610 (elution panel, lane 4 *versus* lane 3). Quantification of ubiquitinated CBX4 in relation
611 to the CBX4 input in shown in Figure 6E. Taken together, these results indicated that

612 SALL1 is able to stabilize CBX4 protein by reducing its ubiquitination and
613 subsequent degradation via the UPS.
614
615 **SALL1 modulates the number and size of CBX4-containing Pc bodies, as well as**
616 **the expression of CBX4 target genes**
617 Although SALL1 does not colocalize with CBX4 in Pc bodies, the finding that
618 SALL1 modulates CBX4 protein levels prompted us to investigate a potential effect
619 of SALL1 expression on CBX4-containing Pc bodies. We transiently transfected
620 SALL1-YFP or its mutant SALL1ΔSUMO-YFP in U2OS cells. GFP-β-Gal was
621 transfected as control. Transfected cells were stained with a specific CBX4 primary
622 antibody and the number and area of CBX4-containing Pc bodies were examined in
623 more than 100 cells per condition (Figure S6). Using confocal microscopy and image
624 analysis with Fiji software (Figure 7A, B), we observed that Pc bodies were
625 significantly larger and more abundant in cells expressing SALL1 or SALL1ΔSUMO
626 than in cells expressing β-Gal. No significant differences in the number of bodies
627 were observed between cells expressing SALL1 and SALL1ΔSUMO. However, the
628 area of the Pc bodies was significantly smaller in SALL1ΔSUMO compared to
629 SALL1 transfected cells. These results revealed that SALL1 SUMOylation status
630 does not influence the increase in the number of Pc bodies, but it may influence their
631 size.
632 Finally, since SALL1 increases CBX4 protein levels, as well as the size and
633 number of Pc bodies, and increased formation of Pc bodies may lead to stronger
634 transcriptional repression of several PRC1 target genes (Gonzalez et al., 2014;
635 Soshnikova, 2014; Cheutin and Cavalli, 2018), we hypothesized that SALL1

636 overexpression could lead to a stronger transcriptional repression of CBX4 targets,
637 including HOX genes.

638 To test this possibility, HEK 293FT cells were transiently transfected with
639 SALL1-YFP, SALL1ΔSUMO-YFP or GFP-β-Gal as control, and the expression
640 levels of several direct CBX4 target genes *(HOXA11*, *HOXB4*, *HOXB7*, *HOXB13*,
641 *HOXC6*, *HOXC10*, *HOXC12*, *HOXD13* and *GATA4)* were analyzed by RT-qPCR.
642 Significant differences in the expression of *HOXB4*, *HOXB13*, *HOXC6*, *HOXC10* and
643 *GATA4* were observed between wild-type SALL1 and β-Gal expressing control cells
644 (Figure 7C). However, no significant differences were observed between
645 SALL1ΔSUMO-transfected cells and control cells.

646 Taken together, these results indicate that high SALL1 levels modulate the
647 transcriptional repression capacity of CBX4 on some of its target genes. Interestingly,
648 SUMOylation of SALL1 seemed to be necessary for this transcriptional effect.

649

650

DISCUSSION

In this work, we have confirmed that SALL1 and CBX4 proteins interact with each other. Although both proteins can be SUMOylated and contain validated (CBX4 (Merrill et al., 2010)) or predicted (SALL1) SIM motifs, our results suggest that the SALL1/CBX4 interaction does not depend on the SUMOylation status of SALL1, nor the mutation of its putative SIMs. We note the possible contribution of the endogenous SALL1 to the interaction, as dimers with the endogenous WT SALL1 and exogenous mutants could be formed, bridging the interaction of mutant SALL1 with CBX4.

Neither SALL1 WT nor the SALL1ΔSUMO or SALL1ΔSIM mutant forms showed colocalization with CBX4 in Pc bodies, a subset of nuclear bodies that have been defined as centers of chromatin regulation for transcriptional repression of target genes (Entrevan et al., 2016). This observation indicates that the SALL1-CBX4 interaction does not occur in this specific cellular compartment. Despite this, we demonstrate that SALL1, as well as its SUMOylation-deficient mutant form, increase the number and size of CBX4-containing Pc bodies. We speculate that a dynamic and transitory interaction with SALL1 in the nucleoplasm may indirectly influence Pc body formation by altering CBX4 levels. In fact, we demonstrated that SALL1 stabilizes and increases CBX4 protein levels in a post-translational manner, reducing its ubiquitination with subsequent reduction of its degradation via the proteasome.

Different hypothetical scenarios could explain the SALL1-mediated stabilization of CBX4. As a transcriptional repressor, SALL1 could inhibit the transcription of ubiquitin E3 ligase(s) involved in CBX4 modification or could facilitate the binding and/or the recognition of CBX4 by DUBs (Ning et al., 2017).

Interestingly, SALL1 was found to interact with members of the UPS, which might disrupt CBX4 homeostasis (Bozal-Basterra et al., 2018). Importantly, we show that high SALL1 levels increase CBX4-mediated transcriptional repression of some of its target genes. Although SUMOylation of SALL1 does not seem to affect its ability to regulate CBX4 protein levels, it seems to be important for SALL1 to modulate CBX4 transcriptional repression activity: only when SALL1 is SUMOylated, the recruitment of CBX4 on the chromatin results in a functional effect. In a speculative scenario, one possible explanation of these results could be the involvement of a third component. For instance, SUMOylation of SALL1 could facilitate the simultaneous interaction with other members of the PRC1, such as RING1 or PHC1. Interestingly, those factors were also found as possible SALL1 interactors in the proximity proteomics analysis that hinted initially to a possible SALL1/CBX4 interaction (Bozal-Basterra et al., 2018). Otherwise, SUMOylation of SALL1 could facilitate the interaction of CBX4 with co-factors required for gene repression (Cheng et al., 2014).

These highly speculative hypotheses can be summarized into the model shown in Figure 8. SALL1 (in its unmodified or SUMOylated form) would interact with CBX4. This interaction would result in less ubiquitination of CBX4 with its consequent stabilization (Figure 8). Thus, CBX4 would be recruited on chromatin, where it would act as a transcriptional repressor of its target genes. In its SUMOylated form, SALL1 could interact, not only with CBX4, but also with repression cofactors or other components of PRC1, which could be recruited on chromatin along with CBX4 (Figure 8, left). The recruitment of transcriptional cofactor(s), or various components of PRC1, would result in the activation of the multiprotein complex with consequent repression of the target genes.

In an alternative hypothesis, SUMOylated SALL1 could enhance CBX4 repression capacity by facilitating its SUMOylation. The SUMOylation of CBX4 is known to be necessary for its repression activity on the chromatin (Kang et al., 2010). We observed that, in the presence of high levels of SALL1, the SUMOylation of CBX4 increased (data not shown). However, this was probably the result of increasing the total levels of the protein. In addition, SALL1 was demonstrated to interact with UBC9 and SUMO1 in a yeast two-hybrid system (Netzer et al., 2002). Interestingly, some members of the SUMOylation pathway were also found in the proximity proteomics analysis of SALL1 (Bozal-Basterra et al., 2018). In this alternative hypothetical scenario, once SUMOylated SALL1 promotes CBX4 stabilization impairing its ubiquitination, it would be able also to promote CBX4 SUMOylation by recruiting an E3 SUMO ligase or other components of the SUMOylation machinery (Figure 8, right). In this regard, the K224 residue involved in CBX4 SUMOylation, and the adjacent K209 and K247 residues were predicted as putative ubiquitination sites by UbPred (http://www.ubpred.org/). This raises the interesting possibility that modification of CBX4 by ubiquitin and SUMO would be mutually exclusive events. Whether this is the case, and whether SALL1 is involved in this regulation, would require further investigation.

Additional experiments are necessary to further test the non-mutually exclusive hypotheses for SALL1-mediated regulation of CBX4. Our results suggest that SALL1 plays an important role in the control of the expression of key developmental genes through the post-transcriptional regulation of CBX4. Where and when this regulation takes place *in vivo* during development deserves further investigation.

CONFLICT OF INTEREST

The authors declare that the research was conducted in the absence of any commercial or financial relationships that could be construed as a potential conflict of interest.

AUTHORS CONTRIBUTIONS

I.G., L.P., J.D.S. and R.B. designed experiments and analyzed data. I.G., L.P., J.A.R., J.D.S. and R.B. wrote the manuscript. I.G., L.P., V.M., E.L., C.P., V.L., E.G.-L., M.G. and O.B.-G. developed experimental protocols, performed experiments, and analyzed data. A.C.O.V., A.M.A., J.A.R. and M.S.R. provided scientific resources.

ACKNOWLEDGEMENTS

R.B., M.S.R., A.C.O.V., J.D.S. and O.B.-G. acknowledge funding by the grant 765445-EU (UbiCODE Program). R.B. acknowledges funding by grants BFU2017-84653-P (MINECO/FEDER, EU), SEV-2016-0644 (Severo Ochoa Excellence Program), SAF2017-90900-REDT (UBIRed Program) and IT1165-19 (Basque Country Government). Additional support was provided by the Department of Industry, Tourism, and Trade of the Basque Country Government (Elkartek Research Programs) and by the Innovation Technology Department of the Bizkaia County. A.M.A. acknowledges CIBERehd. We thank Laura Bozal-Basterra and Arkaitz Carracedo (CIC bioGUNE) for their help in data analysis.

DATA AVAILABILITY

748 The data that support the findings of this study are available from the
749 corresponding author upon reasonable request.
750
751
752 **REFERENCES**
753

754 Abedin, M.J., Imai, N., Rosenberg, M.E., and Gupta, S. (2011). Identification and
755 Characterization of Sall1-Expressing Cells Present in the Adult Mouse Kidney.
756 *Nephron Experimental Nephrology* 119(4)**,** e75-e82. doi: 10.1159/000328925.
757 Aillet, F., Lopitz-Otsoa, F., Hjerpe, R., Torres-Ramos, M., Lang, V., and Rodriguez,
758 M.S. (2012). Isolation of ubiquitylated proteins using tandem ubiquitin-binding
759 entities. *Methods Mol Biol* 832**,** 173-183. doi: 10.1007/978-1-61779-474-2_12.
760 Akimov, V., Barrio-Hernandez, I., Hansen, S.V.F., Hallenborg, P., Pedersen, A.K.,
761 Bekker-Jensen, D.B., et al. (2018). UbiSite approach for comprehensive mapping
762 of lysine and N-terminal ubiquitination sites. *Nat Struct Mol Biol* 25(7)**,** 631-640.
763 doi: 10.1038/s41594-018-0084-y.
764 Beauclair, G., Bridier-Nahmias, A., Zagury, J.F., Saib, A., and Zamborlini, A. (2015).
765 JASSA: a comprehensive tool for prediction of SUMOylation sites and SIMs.
766 *Bioinformatics* 31(21)**,** 3483-3491. doi: 10.1093/bioinformatics/btv403.
767 Borozdin, W., Steinmann, K., Albrecht, B., Bottani, A., Devriendt, K., Leipoldt, M.,
768 et al. (2006). Detection of heterozygousSALL1 deletions by quantitative real time
769 PCR proves the contribution of aSALL1 dosage effect in the pathogenesis of
770 Townes-Brocks syndrome. *Human Mutation* 27(2)**,** 211-212. doi:
771 10.1002/humu.9396.
772 Bozal-Basterra, L., Gonzalez-Santamarta, M., Muratore, V., Bermejo-Arteagabeitia,
773 A., Da Fonseca, C., Barroso-Gomila, O., et al. (2020). LUZP1, a novel regulator of
774 primary cilia and the actin cytoskeleton, is a contributing factor in Townes-Brocks
775 Syndrome. *eLife* 9**,** e55957. doi: 10.7554/eLife.55957.
776 Bozal-Basterra, L., Martín-Ruíz, I., Pirone, L., Liang, Y., Sigurðsson, J.O., Gonzalez-
777 Santamarta, M., et al. (2018). Truncated SALL1 Impedes Primary Cilia Function
778 in Townes-Brocks Syndrome. *American Journal of Human Genetics* 102(2)**,** 249-
779 265. doi: 10.1016/j.ajhg.2017.12.017.

780 Buck, A., Archangelo, L., Dixkens, C., and Kohlhase, J. (2000). Molecular cloning,
781 chromosomal localization, and expression of the murine SALL1 ortholog Sall1.
782 *Cytogenetic and Genome Research* 89(3-4)**,** 150-153. doi: 10.1159/000015598.
783 Casanova, J. (1989). Mutations in the *spalt* gene of *Drosophila* cause ectopic
784 expression of Ultrabithorax and Sex combs reduced. *Roux's archives of*
785 *developmental biology: the official organ of the EDBO* 198(3)**,** 137-140. doi:
786 10.1007/BF02438938.
787 Chen, Q., Huang, L., Pan, D., Zhu, L.J., and Wang, Y.-X. (2018). Cbx4 Sumoylates
788 Prdm16 to Regulate Adipose Tissue Thermogenesis. *Cell Reports* 22(11)**,** 2860-
789 2872. doi: 10.1016/j.celrep.2018.02.057.
790 Cheng, B., Ren, X., and Kerppola, T.K. (2014). KAP1 represses differentiation-
791 inducible genes in embryonic stem cells through cooperative binding with PRC1
792 and derepresses pluripotency-associated genes. *Molecular and Cellular Biology*
793 34(11)**,** 2075-2091. doi: 10.1128/MCB.01729-13.
794 Cheutin, T., and Cavalli, G. (2012). Progressive polycomb assembly on H3K27me3
795 compartments generates polycomb bodies with developmentally regulated motion.
796 *PLoS genetics* 8(1)**,** e1002465. doi: 10.1371/journal.pgen.1002465.
797 Cheutin, T., and Cavalli, G. (2018). Loss of PRC1 induces higher-order opening of
798 Hox loci independently of transcription during Drosophila embryogenesis. *Nature*
799 *Communications* 9(1)**,** 3898. doi: 10.1038/s41467-018-05945-4.
800 de Celis, J.F., and Barrio, R. (2009). Regulation and function of Spalt proteins during
801 animal development. *The International Journal of Developmental Biology* 53(8-9-
802 10)**,** 1385-1398. doi: 10.1387/ijdb.072408jd.
803 Entrevan, M., Schuettengruber, B., and Cavalli, G. (2016). Regulation of Genome
804 Architecture and Function by Polycomb Proteins. *Trends in Cell Biology* 26(7)**,**
805 511-525. doi: 10.1016/j.tcb.2016.04.009.
806 Franco, M., Seyfried, N.T., Brand, A.H., Peng, J., and Mayor, U. (2011). A Novel
807 Strategy to Isolate Ubiquitin Conjugates Reveals Wide Role for Ubiquitination
808 during Neural Development. *Molecular & Cellular Proteomics* 10(5)**,**
809 M110.002188. doi: 10.1074/mcp.M110.002188.
810 Galisson, F., Mahrouche, L., Courcelles, M., Bonneil, E., Meloche, S., Chelbi-Alix,
811 M.K., et al. (2011). A Novel Proteomics Approach to Identify SUMOylated
812 Proteins and Their Modification Sites in Human Cells. *Molecular & Cellular*
813 *Proteomics* 10(2)**,** S1-S15. doi: 10.1074/mcp.M110.004796.

814 Golebiowski, F., Matic, I., Tatham, M.H., Cole, C., Yin, Y., Nakamura, A., et al.
815 (2009). System-Wide Changes to SUMO Modifications in Response to Heat
816 Shock. *Science Signaling* 2(72)**,** ra24-ra24. doi: 10.1126/scisignal.2000282.
817 Gonzalez, I., Mateos-Langerak, J., Thomas, A., Cheutin, T., and Cavalli, G. (2014).
818 Identification of regulators of the three-dimensional polycomb organization by a
819 microscopy-based genome-wide RNAi screen. *Molecular Cell* 54(3)**,** 485-499. doi:
820 10.1016/j.molcel.2014.03.004.
821 Gullberg, M., Gustafsdottir, S.M., Schallmeiner, E., Jarvius, J., Bjarnegard, M.,
822 Betsholtz, C., et al. (2004). Cytokine detection by antibody-based proximity
823 ligation. *Proceedings of the National Academy of Sciences* 101(22)**,** 8420-8424.
824 doi: 10.1073/pnas.0400552101.
825 Hendriks, I.A., D'Souza, R.C.J., Yang, B., Verlaan-de Vries, M., Mann, M., and
826 Vertegaal, A.C.O. (2014). Uncovering global SUMOylation signaling networks in
827 a site-specific manner. *Nature Structural & Molecular Biology* 21(10)**,** 927-936.
828 doi: 10.1038/nsmb.2890.
829 Hendriks, I.A., D'Souza, R.C., Chang, J.-G., Mann, M., and Vertegaal, A.C.O.
830 (2015). System-wide identification of wild-type SUMO-2 conjugation sites. *Nature*
831 *Communications* 6(1)**,** 7289. doi: 10.1038/ncomms8289.
832 Hendriks, I.A., and Vertegaal, A.C. (2016). A comprehensive compilation of SUMO
833 proteomics. *Nat Rev Mol Cell Biol* 17(9)**,** 581-595. doi: 10.1038/nrm.2016.81.
834 Hjerpe, R., Aillet, F., Lopitz-Otsoa, F., Lang, V., England, P., and Rodriguez, M.S.
835 (2009). Efficient protection and isolation of ubiquitylated proteins using tandem
836 ubiquitin-binding entities. *EMBO Rep* 10(11)**,** 1250-1258. doi:
837 10.1038/embor.2009.192.
838 Ismail, I.H., Gagné, J.-P., Caron, M.-C., McDonald, D., Xu, Z., Masson, J.-Y., et al.
839 (2012). CBX4-mediated SUMO modification regulates BMI1 recruitment at sites
840 of DNA damage. *Nucleic Acids Research* 40(12)**,** 5497-5510. doi:
841 10.1093/nar/gks222.
842 Kagey, M.H., Melhuish, T.A., and Wotton, D. (2003). The polycomb protein Pc2 is a
843 SUMO E3. *Cell* 113(1)**,** 127-137. doi: 10.1016/s0092-8674(03)00159-4.
844 Kang, X., Qi, Y., Zuo, Y., Wang, Q., Zou, Y., Schwartz, R.J., et al. (2010). SUMO-
845 specific protease 2 is essential for suppression of polycomb group protein-
846 mediated gene silencing during embryonic development. *Molecular Cell* 38(2)**,**
847 191-201. doi: 10.1016/j.molcel.2010.03.005.

Kiefer, S.M., McDill, B.W., Yang, J., and Rauchman, M. (2002). Murine Sall1 represses transcription by recruiting a histone deacetylase complex. *The Journal of Biological Chemistry* 277(17)**,** 14869-14876. doi: 10.1074/jbc.M200052200.

Klauke, K., Radulovic, V., Broekhuis, M., Weersing, E., Zwart, E., Olthof, S., et al. (2013). Polycomb Cbx family members mediate the balance between haematopoietic stem cell self-renewal and differentiation. *Nat Cell Biol* 15(4)**,** 353-362. doi: 10.1038/ncb2701.

Kohlhase, J. (1993). "Townes-Brocks Syndrome," in *GeneReviews((R)),* eds. M.P. Adam, H.H. Ardinger, R.A. Pagon, S.E. Wallace, L.J.H. Bean, G. Mirzaa & A. Amemiya. (Seattle (WA)).

Kohlhase, J., Wischermann, A., Reichenbach, H., Froster, U., and Engel, W. (1998). Mutations in the SALL1 putative transcription factor gene cause Townes-Brocks syndrome. *Nature Genetics* 18(1)**,** 81-83. doi: 10.1038/ng0198-81.

Lamoliatte, F., Caron, D., Durette, C., Mahrouche, L., Maroui, M.A., Caron-Lizotte, O., et al. (2014). Large-scale analysis of lysine SUMOylation by SUMO remnant immunoaffinity profiling. *Nat Commun* 5**,** 5409. doi: 10.1038/ncomms6409.

Landecker, H.L., Sinclair, D.A., and Brock, H.W. (1994). Screen for enhancers of Polycomb and Polycomblike in Drosophila melanogaster. *Developmental Genetics* 15(5)**,** 425-434. doi: 10.1002/dvg.1020150505.

Lauberth, S.M., and Rauchman, M. (2006). A conserved 12-amino acid motif in Sall1 recruits the nucleosome remodeling and deacetylase corepressor complex. *The Journal of Biological Chemistry* 281(33)**,** 23922-23931. doi: 10.1074/jbc.M513461200.

Li, B., Zhou, J., Liu, P., Hu, J., Jin, H., Shimono, Y., et al. (2007). Polycomb protein Cbx4 promotes SUMO modification of de novo DNA methyltransferase Dnmt3a. *The Biochemical Journal* 405(2)**,** 369-378. doi: 10.1042/BJ20061873.

Livak, K.J., and Schmittgen, T.D. (2001). Analysis of relative gene expression data using real-time quantitative PCR and the 2(-Delta Delta C(T)) Method. *Methods* 25(4)**,** 402-408. doi: 10.1006/meth.2001.1262.

MacPherson, M.J., Beatty, L.G., Zhou, W., Du, M., and Sadowski, P.D. (2009). The CTCF Insulator Protein Is Posttranslationally Modified by SUMO. *Molecular and Cellular Biology* 29(3)**,** 714-725. doi: 10.1128/MCB.00825-08.

Mardaryev, A.N., Liu, B., Rapisarda, V., Poterlowicz, K., Malashchuk, I., Rudolf, J., et al. (2016). Cbx4 maintains the epithelial lineage identity and cell proliferation in

the developing stratified epithelium. *J Cell Biol* 212(1), 77-89. doi: 10.1083/jcb.201506065.

Matic, I., Schimmel, J., Hendriks, I.A., van Santen, M.A., van de Rijke, F., van Dam, H., et al. (2010). Site-Specific Identification of SUMO-2 Targets in Cells Reveals an Inverted SUMOylation Motif and a Hydrophobic Cluster SUMOylation Motif. *Molecular Cell* 39(4), 641-652. doi: 10.1016/j.molcel.2010.07.026.

Merrill, J.C., Melhuish, T.A., Kagey, M.H., Yang, S.-H., Sharrocks, A.D., and Wotton, D. (2010). A Role for Non-Covalent SUMO Interaction Motifs in Pc2/CBX4 E3 Activity. *PLoS ONE* 5(1), e8794. doi: 10.1371/journal.pone.0008794.

Mertins, P., Qiao, J.W., Patel, J., Udeshi, N.D., Clauser, K.R., Mani, D.R., et al. (2013). Integrated proteomic analysis of post-translational modifications by serial enrichment. *Nat Methods* 10(7), 634-637. doi: 10.1038/nmeth.2518.

Netzer, C., Bohlander, S.K., Rieger, L., Müller, S., and Kohlhase, J. (2002). Interaction of the developmental regulator SALL1 with UBE2I and SUMO-1. *Biochemical and Biophysical Research Communications* 296(4), 870-876. doi: 10.1016/s0006-291x(02)02003-x.

Netzer, C., Rieger, L., Brero, A., Zhang, C.D., Hinzke, M., Kohlhase, J., et al. (2001). SALL1, the gene mutated in Townes-Brocks syndrome, encodes a transcriptional repressor which interacts with TRF1/PIN2 and localizes to pericentromeric heterochromatin. *Hum Mol Genet* 10(26), 3017-3024. doi: 10.1093/hmg/10.26.3017.

Ning, B., Zhao, W., Qian, C., Liu, P., Li, Q., Li, W., et al. (2017). USP26 functions as a negative regulator of cellular reprogramming by stabilising PRC1 complex components. *Nature Communications* 8(1), 349. doi: 10.1038/s41467-017-00301-4.

Pelisch, F., Pozzi, B., Risso, G., Muñoz, M.J., and Srebrow, A. (2012). DNA Damage-induced Heterogeneous Nuclear Ribonucleoprotein K SUMOylation Regulates p53 Transcriptional Activation. *Journal of Biological Chemistry* 287(36), 30789-30799. doi: 10.1074/jbc.M112.390120.

Pirone, L., Xolalpa, W., Mayor, U., Barrio, R., and Sutherland, J.D. (2016). Analysis of SUMOylated Proteins in Cells and In Vivo Using the bioSUMO Strategy. *Methods Mol Biol* 1475, 161-169. doi: 10.1007/978-1-4939-6358-4_12.

915 Pirone, L., Xolalpa, W., Sigurðsson, J.O., Ramirez, J., Pérez, C., González, M., et al.
916 (2017). A comprehensive platform for the analysis of ubiquitin-like protein
917 modifications using in vivo biotinylation. *Scientific Reports* 7**,** 40756. doi:
918 10.1038/srep40756.
919 Povlsen, L.K., Beli, P., Wagner, S.A., Poulsen, S.L., Sylvestersen, K.B., Poulsen,
920 J.W., et al. (2012). Systems-wide analysis of ubiquitylation dynamics reveals a key
921 role for PAF15 ubiquitylation in DNA-damage bypass. *Nat Cell Biol* 14(10)**,** 1089-
922 1098. doi: 10.1038/ncb2579.
923 Ren, X., Hu, B., Song, M., Ding, Z., Dang, Y., Liu, Z., et al. (2019). Maintenance of
924 Nucleolar Homeostasis by CBX4 Alleviates Senescence and Osteoarthritis. *Cell*
925 *Reports* 26(13)**,** 3643-3656.e3647. doi: 10.1016/j.celrep.2019.02.088.
926 Roux, K.J., Kim, D.I., and Burke, B. (2013). BioID: a screen for protein-protein
927 interactions. *Curr Protoc Protein Sci* 74**,** 19 23 11-19 23 14. doi:
928 10.1002/0471140864.ps1923s74.
929 Sánchez, J., Talamillo, A., González, M., Sánchez-Pulido, L., Jiménez, S., Pirone, L.,
930 et al. (2011). Drosophila Sal and Salr are transcriptional repressors. *The*
931 *Biochemical Journal* 438(3)**,** 437-445. doi: 10.1042/BJ20110229.
932 Sánchez, J., Talamillo, A., Lopitz-Otsoa, F., Pérez, C., Hjerpe, R., Sutherland, J.D., et
933 al. (2010). Sumoylation modulates the activity of Spalt-like proteins during wing
934 development in Drosophila. *The Journal of Biological Chemistry* 285(33)**,** 25841-
935 25849. doi: 10.1074/jbc.M110.124024.
936 Saurin, A.J., Shiels, C., Williamson, J., Satijn, D.P., Otte, A.P., Sheer, D., et al.
937 (1998). The human polycomb group complex associates with pericentromeric
938 heterochromatin to form a novel nuclear domain. *The Journal of Cell Biology*
939 142(4)**,** 887-898. doi: 10.1083/jcb.142.4.887.
940 Schimmel, J., Eifler, K., Sigurðsson, Jón O., Cuijpers, Sabine A.G., Hendriks, Ivo A.,
941 Verlaan-de Vries, M., et al. (2014). Uncovering SUMOylation Dynamics during
942 Cell-Cycle Progression Reveals FoxM1 as a Key Mitotic SUMO Target Protein.
943 *Molecular Cell* 53(6)**,** 1053-1066. doi: 10.1016/j.molcel.2014.02.001.
944 Schuettengruber, B., Bourbon, H.-M., Di Croce, L., and Cavalli, G. (2017). Genome
945 Regulation by Polycomb and Trithorax: 70 Years and Counting. *Cell* 171(1)**,** 34-
946 57. doi: 10.1016/j.cell.2017.08.002.
947 Söderberg, O., Gullberg, M., Jarvius, M., Ridderstråle, K., Leuchowius, K.-J., Jarvius,
948 J., et al. (2006). Direct observation of individual endogenous protein complexes in

949 situ by proximity ligation. *Nature Methods* 3(12), 995-1000. doi:
950 10.1038/nmeth947.
951 Soria-Bretones, I., Cepeda-García, C., Checa-Rodriguez, C., Heyer, V., Reina-San-
952 Martin, B., Soutoglou, E., et al. (2017). DNA end resection requires constitutive
953 sumoylation of CtIP by CBX4. *Nature Communications* 8(1), 113. doi:
954 10.1038/s41467-017-00183-6.
955 Soshnikova, N. (2014). Hox genes regulation in vertebrates. *Developmental*
956 *Dynamics: An Official Publication of the American Association of Anatomists*
957 243(1), 49-58. doi: 10.1002/dvdy.24014.
958 Sweetman, D., Smith, T., Farrell, E.R., Chantry, A., and Munsterberg, A. (2003). The
959 conserved glutamine-rich region of chick csal1 and csal3 mediates protein
960 interactions with other spalt family members. Implications for Townes-Brocks
961 syndrome. *The Journal of Biological Chemistry* 278(8), 6560-6566. doi:
962 10.1074/jbc.M209066200.
963 Tammsalu, T., Matic, I., Jaffray, E.G., Ibrahim, A.F.M., Tatham, M.H., and Hay, R.T.
964 (2014). Proteome-wide identification of SUMO2 modification sites. *Sci Signal*
965 7(323), rs2. doi: 10.1126/scisignal.2005146.
966 Udeshi, N.D., Svinkina, T., Mertins, P., Kuhn, E., Mani, D.R., Qiao, J.W., et al.
967 (2013). Refined preparation and use of anti-diglycine remnant (K-epsilon-GG)
968 antibody enables routine quantification of 10,000s of ubiquitination sites in single
969 proteomics experiments. *Mol Cell Proteomics* 12(3), 825-831. doi:
970 10.1074/mcp.O112.027094.
971 Wang, X., Li, L., Wu, Y., Zhang, R., Zhang, M., Liao, D., et al. (2016). CBX4
972 Suppresses Metastasis via Recruitment of HDAC3 to the Runx2 Promoter in
973 Colorectal Carcinoma. *Cancer Research* 76(24), 7277-7289. doi: 10.1158/0008-
974 5472.CAN-16-2100.
975 Wang, X., Qin, G., Liang, X., Wang, W., Wang, Z., Liao, D., et al. (2020). Targeting
976 the CK1α/CBX4 axis for metastasis in osteosarcoma. *Nature Communications*
977 11(1), 1141. doi: 10.1038/s41467-020-14870-4.
978 Wotton, D., and Merrill, J.C. (2007). Pc2 and SUMOylation. *Biochem Soc Trans*
979 35(Pt 6), 1401-1404. doi: 10.1042/BST0351401.
980 Xiao, Z., Chang, J.-G., Hendriks, I.A., Sigurðsson, J.O., Olsen, J.V., and Vertegaal,
981 A.C.O. (2015). System-wide Analysis of SUMOylation Dynamics in Response to
982 Replication Stress Reveals Novel Small Ubiquitin-like Modified Target Proteins

and Acceptor Lysines Relevant for Genome Stability. *Molecular & Cellular Proteomics* 14(5)**,** 1419-1434. doi: 10.1074/mcp.O114.044792.

Zhao, Q., Xie, Y., Zheng, Y., Jiang, S., Liu, W., Mu, W., et al. (2014). GPS-SUMO: a tool for the prediction of sumoylation sites and SUMO-interaction motifs. *Nucleic Acids Research* 42(W1)**,** W325-W330. doi: 10.1093/nar/gku383.

Zidovska, A. (2020). The rich inner life of the cell nucleus: dynamic organization, active flows, and emergent rheology. *Biophys Rev* 12(5)**,** 1093-1106. doi: 10.1007/s12551-020-00761-x.

FIGURE LEGENDS

Figure 1. SALL1 and CBX4 do not colocalize in nuclear bodies. (A-F) Confocal images of U2OS cells showing expression of SALL1-YFP, SALL1ΔSUMO-YFP or SALL1ΔSIM-YFP (green), and endogenous CBX4 (magenta in **A-C**) or endogenous SUMO2/3 (magenta in **D-F**). Nuclei were stained with DAPI. Black and white pictures show single green or magenta channels. Green arrowheads indicate SALL1 bodies, magenta arrowheads indicate Pc bodies (in **A-C**), or SUMO bodies (in **D-F**) and white arrowheads indicate colocalization of SALL1 and SUMO2/3 (in **D-F**). Pictures were taken with a Leica DM IRE2 confocal microscope using a 63X objective. Scale bars indicate 5 micrometers.

Figure 2. SALL1 interacts with CBX4 in a SUMOylation-independent manner. (A) Validation of the interaction between human SALL1 and human CBX4 or *Drosophila melanogaster* Pc proteins using BioID-based biotin pulldown in transfected HEK 293FT cells. In the Input panel, the relative expression of the HA-tagged SALL1 proteins (the full-length protein or a TBS-related truncation mutant) is shown. One asterisk indicates SALL1-HA, while two asterisks indicate $SALL1^{826}$-HA. Negative controls (single expression of each individual protein) are shown in lanes 4-7. Anti-GAPDH was used as loading control. As shown in the Elution panel, CBX4-BirA* interact preferentially with full-length SALL1-HA (lane 1). Anti-biotin blot shows the efficiency of the different pulldowns. **(B)** Validation of the interaction between SALL1 and CBX4 using GFP-Trap. The Input panel shows the expression of epitope-tagged SALL1 and CBX4 proteins in transfected HEK 293FT cells. YFP alone and HA empty vector were used as controls. Lanes 1 and 2 of the Elution panel,

show that CBX4 interacts with SALL1 full length and the truncated form. **(C)** SUMO-related SALL1 mutants interact with CBX4. Western blot analysis of proteins extracted from HEK 293FT cells transfected with the indicated plasmids. Pulldowns were performed using GFP-Trap. As shown in the Elution panel, (lanes 4, 5, and 6), interaction between CBX4 and WT SALL1 or SALL1 mutants was readily detected in all blot images. **(D)** Graph showing that CBX4 levels increase when co-expressed with WT SALL1-YFP, SALL1ΔSUMO-YFP or SALL1ΔSIM-YFP. The intensity of CBX4 bands in blots was quantified using ImageJ, normalized to β-Actin and reported as fold change relative to the YFP alone control. The mean plus SEM of 3 independent experiments is plotted. P-values were calculated using Mann Whitney test. (*) P-value < 0.05. **(A, B, C)** Antibodies used are indicated to the left. Molecular weight markers are indicated to the right in KDa.

Figure 3. SALL1 and CBX4 interact in the nucleoplasm. (A-D) Confocal pictures of a proximity ligation assay (PLA) showing *in situ* interaction of SALL1 and CBX4 in the nucleus of U2OS cells, visualized as magenta spots. Cells were transfected with SALL1-HA or with the empty pcDNA3 vector as negative control. Antibodies used in the assay are indicated in magenta. Panel **A** shows SALL1 and CBX4 interaction, while panels **B-D** are negative controls. **(E)** Quantification of PLA signals per cell as in panels **A-D**. Bars represent mean plus SEM of 3 independent experiments. P-values were calculated using One-way ANOVA test. (***) P-value < 0.001.

Figure 4. SALL1 influences the levels of CBX4. (A) Western blot showing protein levels of CBX4-HA when co-expressed with SALL1-YFP or YFP alone in HEK 293FT cells. Actin expression was used as loading control. **(B)** Western blot showing

expression levels of endogenous CBX4 protein in parental HEK 293FT cells (lane 1) or in HEK 293FT cells stably expressing GFS-SALL1 (lane 2). **(C)** Confocal microscopy images showing inducible expression SALL1-2xHA in HEK 293FT_TripZ-SALL1-2xHA cells. Cells were treated with different concentrations of doxycycline (Dox) to induce SALL1 expression as indicated. SALL1-2xHA was detected using anti-SALL1 primary antibody (green). Cell nuclei were stained with DAPI (blue). **(D)** Western blot analysis showing expression levels of endogenous CBX4 in HEK 293FT_TripZ-SALL1-2xHA cells treated with increasing concentrations of Dox. **(E)** Quantification of the expression levels of endogenous CBX4 in HEK 293FT_TripZ-SALL1-2xHA cells treated with increasing concentrations of Dox. Three independent experiments as the one shown in panel D were performed. The intensity of CBX4 bands was quantified using ImageJ, and the values were normalized to the levels of Actin. P-value was calculated using One-way ANOVA test. (*) P-value < 0.05. **(F)** RT-qPCR analysis of *SALL1* and *CBX4* mRNA expression in HEK 293FT_TripZ-SALL1-2xHA cells treated with increasing concentrations of Dox. SALL1 and CBX4 expression were normalized using *GAPDH* expression and shown as fold change relative to untreated control. **(A, B, D)** Molecular weight markers are shown to the right in KDa. Antibodies were used as indicated to the left. **(E, F)** The mean plus SEM of at least three independent experiments is shown.

Figure 5. SALL1 stabilizes CBX4 protein. (A, C) Western blot analysis of cycloheximide (CHX) chase experiments performed in HEK 293FT cells transfected with *SALL1-YFP*, *SALL1ΔSUMO-YFP* or *GFP-β-Gal*. Cells were treated with 50 μg/ml of CHX in the absence (**A**) or presence (**C**) of 10 μM of the proteasome

inhibitor MG132. Cells were collected at different time points (0, 4, 8 and 16 hours after initiation of treatment) and endogenous CBX4 levels were analyzed by Western blot. Vinculin was used as loading control. Molecular weight markers are shown to the right in KDa. Antibodies were used as indicated to the left. (**B, D)** CBX4 levels were quantified after CHX treatment alone (**B**) or in combination with MG132 (**D**), normalized to Vinculin, and data from six different independent experiments were pooled together. Graphs show mean plus SEM. P-values were calculated using One-way ANOVA test. (*) P-value < 0.05; (**) P-value < 0.01.

Figure 6. CBX4 ubiquitination is reduced in presence of SALL1. (A) Western blot analysis of HEK 293FT cells transfected with *CBX4-HA* together with *CMV-BirA-2A-bioUb* or *BirA* as a negative control. Cells were treated with 50 μM of biotin in the presence or absence of 10 μM MG132. Protein lysates were subjected to pulldown with streptavidin beads and the results were analyzed by Western blot. Two asterisks indicate monoubiquitinated CBX4-HA protein and the vertical line indicates the polyubiquitination smear. **(B)** Western blot analysis of HEK 293FT_TripZ-SALL1-2xHA cells transiently transfected with *CBX4-YFP* together with *BirA-2A-bioUb* or *BirA* as control. The cells were treated or not with 1 μg/ml of doxycycline (Dox), in presence or absence of 10 μM of MG132. Protein lysates were incubated with streptavidin beads to isolate bioUb conjugated proteins and results were analyzed by Western blot. β-Actin was used as loading control. **(C)** The levels of ubiquitinated CBX4-YFP in Dox induced and not induced cells, in presence (right panel) or absence (left panel) of MG132, were quantified and normalized to the CBX4 levels in the input**. (D)** Western blot analysis of endogenous CBX4 in HEK 293FT cells transfected with *CMV-SALL1-2xHA* (lanes 2 and 4) or with pcDNA3 control plasmid

(lanes 1 and 3), in presence (lanes 3 and 4) or absence (lanes 1 and 2) of 10 μM MG132. **(E)** Quantification of ubiquitinated CBX4 in the elution panel normalized to the CBX4 levels in the input, in cells expressing or not SALL1-HA, in presence (right panel) or absence (left panel) of MG132. **(A, B, D)** Molecular weight markers are shown to the right in KDa. Antibodies were used as indicated to the left. **(C, E)** Graphs represent mean plus SEM. P-values were calculated on n= 4 using Mann Whitney test. (*) P-value < 0.05.

Figure 7. SALL1 expression increases the number and size of CBX4-containing Pc bodies and enhances downregulation of CBX4 targets. (A, B) Graphs represent the number of CBX4-containing Pc bodies (**A**) and their mean area in pixels quantified using Fiji software (**B**) in U2OS cells expressing SALL1-YFP, SALL1ΔSUMO-YFP or GFP-β–Gal as a negative control. **(C)** Graph showing the mRNA expression levels of several CBX4 target genes in HEK 293FT cells expressing SALL1-YFP, SALL1ΔSUMO-YFP or GFP-β-Gal as control. Data shown correspond to the mean plus SEM of at least 5 independent RT-qPCR experiments. Gene expression data were normalized to *GAPDH* and are shown as relative fold change over β-Gal expressing cells (magenta line). P-values were calculated using One-way ANOVA test. (*) P-value < 0.05; (**) P-value < 0.01.

Figure 8. SALL1 influences regulation of CBX4 target genes. Hypothetical model showing speculative scenarios whereby SALL1 could influence CBX4-mediated regulation of target genes. Binding to SALL1 (SUMOylated or non-SUMOylated) could stabilize CBX4 by interfering with its ubiquitination and its consequent degradation by the proteasome. CBX4 stabilization entails an increment of its protein

levels and its accumulation in Pc bodies. Binding to SUMOylated SALL1 increases CBX4-mediated transcriptional repression of its target genes. At least two non-exclusive hypothetical mechanisms might underlie this effect. Under one hypothetical scenario (left side), it could be due to the concurrent recruitment of other essential cofactors. In another hypothetical scenario (right side), SUMOylated SALL1 could increase CBX4 transcriptional repression by facilitating its SUMOylation through recruitment of SUMOylation machinery components. Discontinuous arrows indicate speculative events that have not been proven experimentally.

SUPPLEMENTARY FIGURES

Supplementary Figure S1. SALL1 localizes to nuclear bodies. Endogenous SALL1 **(A)** and transiently expressed SALL1-YFP **(B)** localize to nuclear bodies in U2OS cells. In contrast, YFP alone, used as a control, shows a homogenous distribution in the nucleus and cytoplasm **(C)**. Pictures were taken with an AxioD Fluorescent microscope using 100X objective. Scale bars indicate 5 micrometers.

Supplementary Figure S2. Characterization of CBX4 and SALL1 nuclear bodies. (A-D) Endogenous CBX4 (green) does not colocalize with SUM2/3, SUMO1, nor PML bodies or with SC35 (magenta) in U2OS cells. (**E-I)** SALL1-YFP (green) partially colocalizes with endogenous SUMO1 (magenta) in U2OS cells **(E)**. Similar results were obtained for the SALL1ΔSUMO and SALL1ΔSIM mutants **(F, G)**. SALL1 does not colocalize with PML **(H)** nor with SC35 **(I)**. Green and magenta channels are shown independently in black and white. Nuclei were stained with DAPI

(blue). White arrowheads indicate colocalization, green arrowheads indicate domains where mainly CBX4 **(A-D)** or SALL1 **(E-I)** proteins are present, magenta arrowheads indicate domains where mainly SUMO2 **(A)**, SUMO1 **(B, E-G)**, PML **(C, H)** or SC35 **(D, I)** are present. Pictures were taken using a Leica DM IRE2 confocal microscope with a 63X objective, except for pictures in C that were taken using an AxioD Fluorescent microscope and objective 40X. Scale bars indicate 5 micrometers.

Supplementary Figure S3. SALL1 SUMOylation sites and SIMs are conserved throughout evolution. (A) SALL1 schematic representation. Ovals represent the zinc fingers (ZF) distributed along the protein. Blue rectangle represents the poly-glutamine (PQ) domain. In magenta, SUMO consensus sites mutated in SALL1ΔSUMO and, in blue, predicted SIMs mutated in SALL1ΔSIM. **(B)** SALL1 fused to HA tag was SUMOylated in the presence (black circles) of bioSUMO3, transiently transfected in HEK 293FT cells. Asterisks indicate the modified SALL1 (SUMO-SALL1) that is shifted if compared with the size of non-modified SALL1 (arrowhead). Anti-tubulin staining was used as a loading control. Molecular weight markers are shown to the right in KDa. SALL1ΔSUMO fused to HA tag is not SUMOylated in presence of bioSUMO3. In the input the expression of WT and SUMO mutant of SALL1 are shown. **(C)** In magenta, SUMO consensus sites in SALL1 that were mutated in SALL1ΔSUMO and, in blue, the predicted SIMs of SALL1, mutated in SALL1ΔSIM mutant. **(D)** Evolutionary conservation of the SUMOylation and SIM sites in SALL1 homologues in the indicated species. Asterisks indicate identical residues, colons and semicolons indicate conservative and semi-conservative changes, respectively.

Supplementary Figure S4. CBX4 and SALL1 localize to the nucleoplasm. Endogenous CBX4 **(A)** and endogenous SALL1 **(B)** shown in green localize to nuclear bodies in U2OS cells **(A', B')**. Increasing the intensity reveals the localization of both proteins in the nucleoplasm **(A'', B'')**. Single green channels are shown in black and white. Pictures were taken using a Leica DM IRE2 confocal microscope with a 63X objective.

Supplementary Figure S5. SALL1 SUMOylation is independent of CBX4. *In vitro* SUMOylation of SALL1 with SUMO1 or SUMO2/3 in the presence of growing quantities of CBX4 (in µl). Wheat germ was added as negative control. The vertical bar indicates the SUMOylated forms of SALL1, the empty arrowhead indicates the unmodified SALL1. Molecular weight markers are shown to the right in KDa.

Supplementary Figure S6. Variation of Polycomb bodies upon SALL1 expression. Representative composition of independent U2OS cells transfected with equal amounts of SALL1-YFP, SALL1ΔSUMO-YFP or GFP-β–Gal plasmids, stained for endogenous CBX4. Nuclei were labelled with DAPI (not shown). Pictures were taken using a Leica DM IRE2 confocal microscope with a 63X objective, using the same settings for all the conditions.

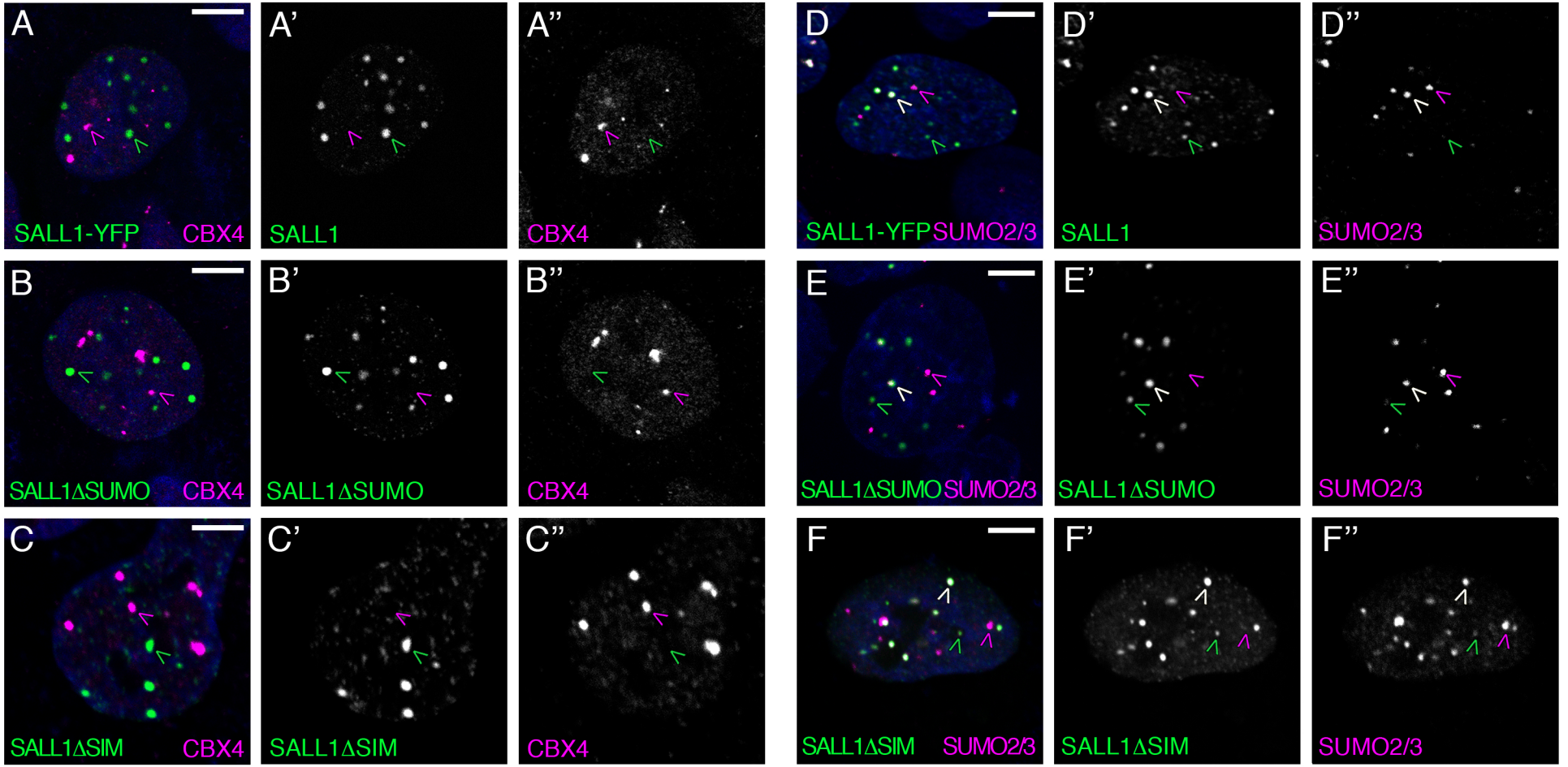
A
A'
A''
SALL1-YFP
CBX4
SALL1
CBX4
B
B'
B''
SALL1ΔSUMO
CBX4
SALL1ΔSUMO
CBX4
C
C'
C''
SALL1ΔSIM
CBX4
SALL1ΔSIM
CBX4
D
D'
D''
SALL1-YFP
SUMO2/3
SALL1
SUMO2/3
E
E'
E''
SALL1ΔSUMO
SUMO2/3
SALL1ΔSUMO
SUMO2/3
F
F'
F''
SALL1ΔSIM
SUMO2/3
SALL1ΔSIM
SUMO2/3

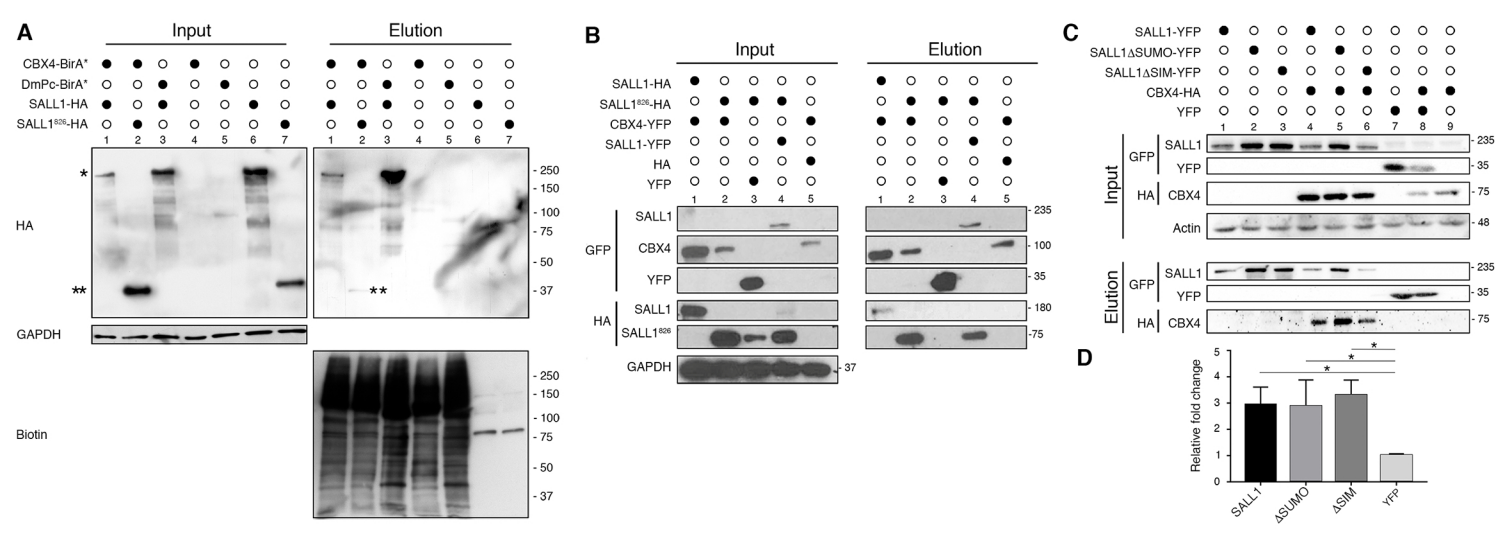
A
Input
Elution
CBX4-BirA*
DmPc-BirA*
SALL1-HA
SALL1826-HA
1 2 3 4 5 6 7
HA
GAPDH
Biotin
250
150
100
75
50
37
B
Input
Elution
SALL1-HA
SALL1826-HA
CBX4-YFP
SALL1-YFP
HA
YFP
1 2 3 4 5
GFP
SALL1
CBX4
YFP
HA
SALL1826
GAPDH
235
100
35
180
75
37
C
SALL1-YFP
SALL1ΔSUMO-YFP
SALL1ΔSIM-YFP
CBX4-HA
YFP
1 2 3 4 5 6 7 8 9
Input
Elution
GFP
HA
SALL1
YFP
CBX4
Actin
235
35
75
48
D
Relative fold change
0 1 2 3 4 5
SALL1
ΔSUMO
ΔSIM
YFP

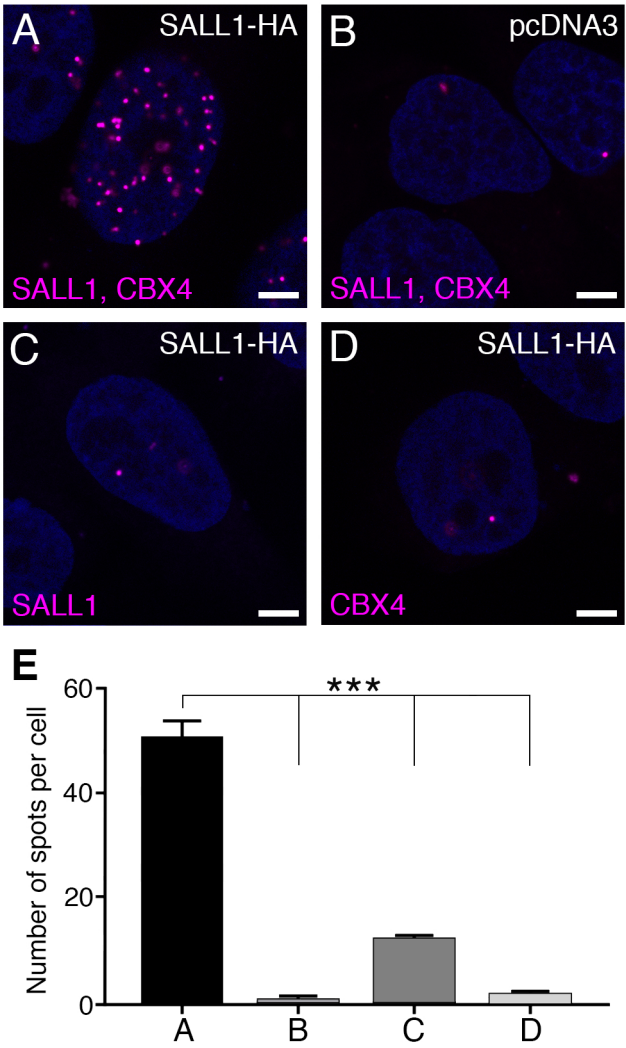
A
SALL1-HA
SALL1, CBX4
B
pcDNA3
SALL1, CBX4
C
SALL1-HA
SALL1
D
SALL1-HA
CBX4
E
***
Number of spots per cell
60
40
20
0
A
B
C
D

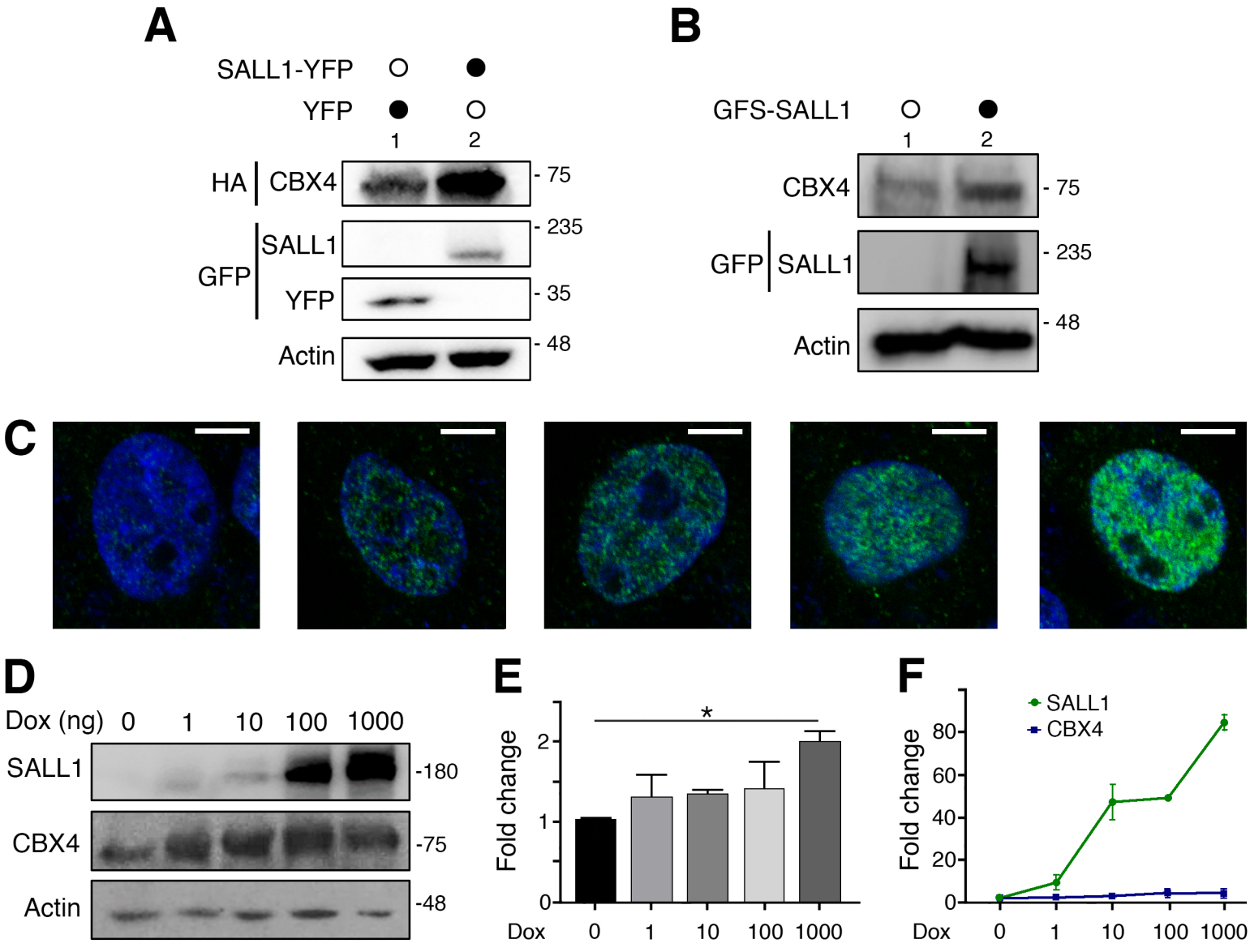
A
SALL1-YFP
YFP
1
2
HA
CBX4
GFP
SALL1
YFP
Actin
75
235
35
48
B
GFS-SALL1
1
2
CBX4
GFP
SALL1
Actin
75
235
48
C
D
Dox (ng) 0 1 10 100 1000
SALL1
CBX4
Actin
-180
-75
-48
E
Fold change
*
Dox 0 1 10 100 1000
F
SALL1
CBX4
Fold change
Dox 0 1 10 100 1000

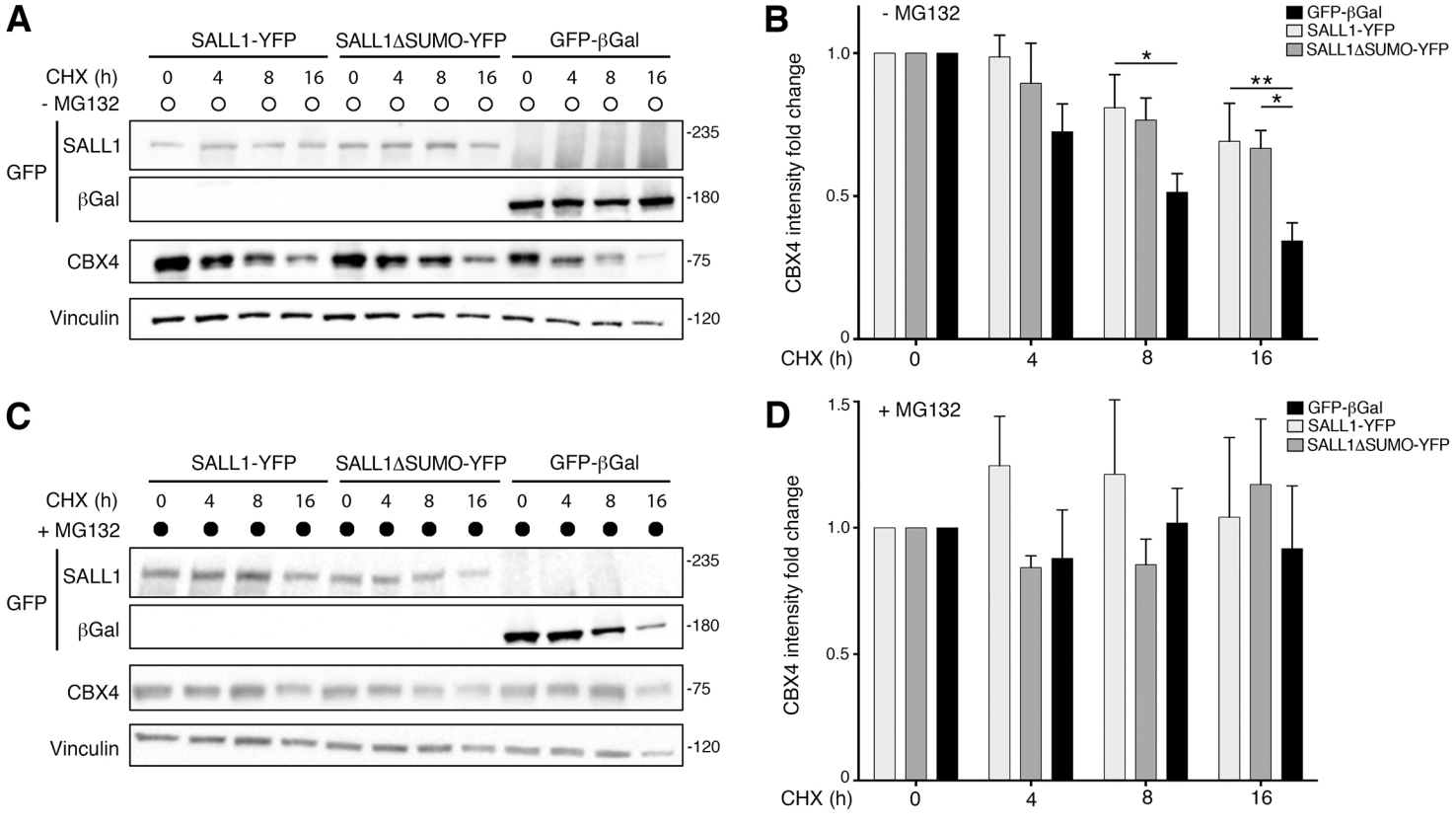
A
SALL1-YFP
SALL1ΔSUMO-YFP
GFP-βGal
CHX (h)
0 4 8 16 0 4 8 16 0 4 8 16
- MG132
GFP
SALL1
βGal
CBX4
Vinculin
-235
-180
-75
-120
B
- MG132
GFP-βGal
SALL1-YFP
SALL1ΔSUMO-YFP
CBX4 intensity fold change
1.0
0.5
0
*
**
*
CHX (h)
0
4
8
16
C
SALL1-YFP
SALL1ΔSUMO-YFP
GFP-βGal
CHX (h)
0 4 8 16 0 4 8 16 0 4 8 16
+ MG132
GFP
SALL1
βGal
CBX4
Vinculin
-235
-180
-75
-120
D
+ MG132
GFP-βGal
SALL1-YFP
SALL1ΔSUMO-YFP
CBX4 intensity fold change
1.5
1.0
0.5
0
CHX (h)
0
4
8
16

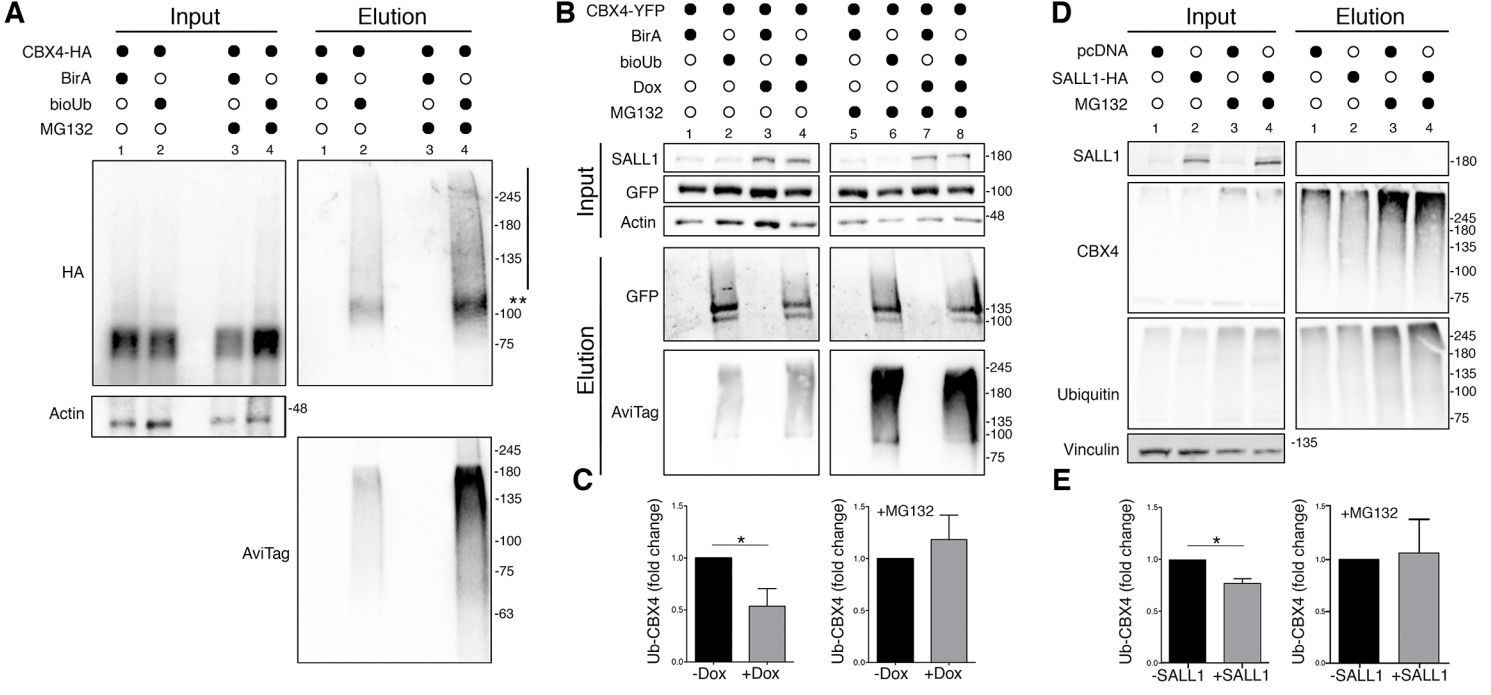
A
Input
Elution
CBX4-HA
BirA
bioUb
MG132
1 2 3 4
1 2 3 4
HA
Actin
AviTag
245
180
135
100
75
63
48
**
B
CBX4-YFP
BirA
bioUb
Dox
MG132
1 2 3 4 5 6 7 8
Input
Elution
SALL1
GFP
Actin
GFP
AviTag
180
100
48
135
100
245
180
135
100
75
C
Ub-CBX4 (fold change)
1.5
1.0
0.5
0.0
*
-Dox +Dox
+MG132
-Dox +Dox
D
Input
Elution
pcDNA
SALL1-HA
MG132
1 2 3 4
1 2 3 4
SALL1
CBX4
Ubiquitin
Vinculin
180
245
180
135
100
75
135
E
Ub-CBX4 (fold change)
*
-SALL1 +SALL1
+MG132
-SALL1 +SALL1

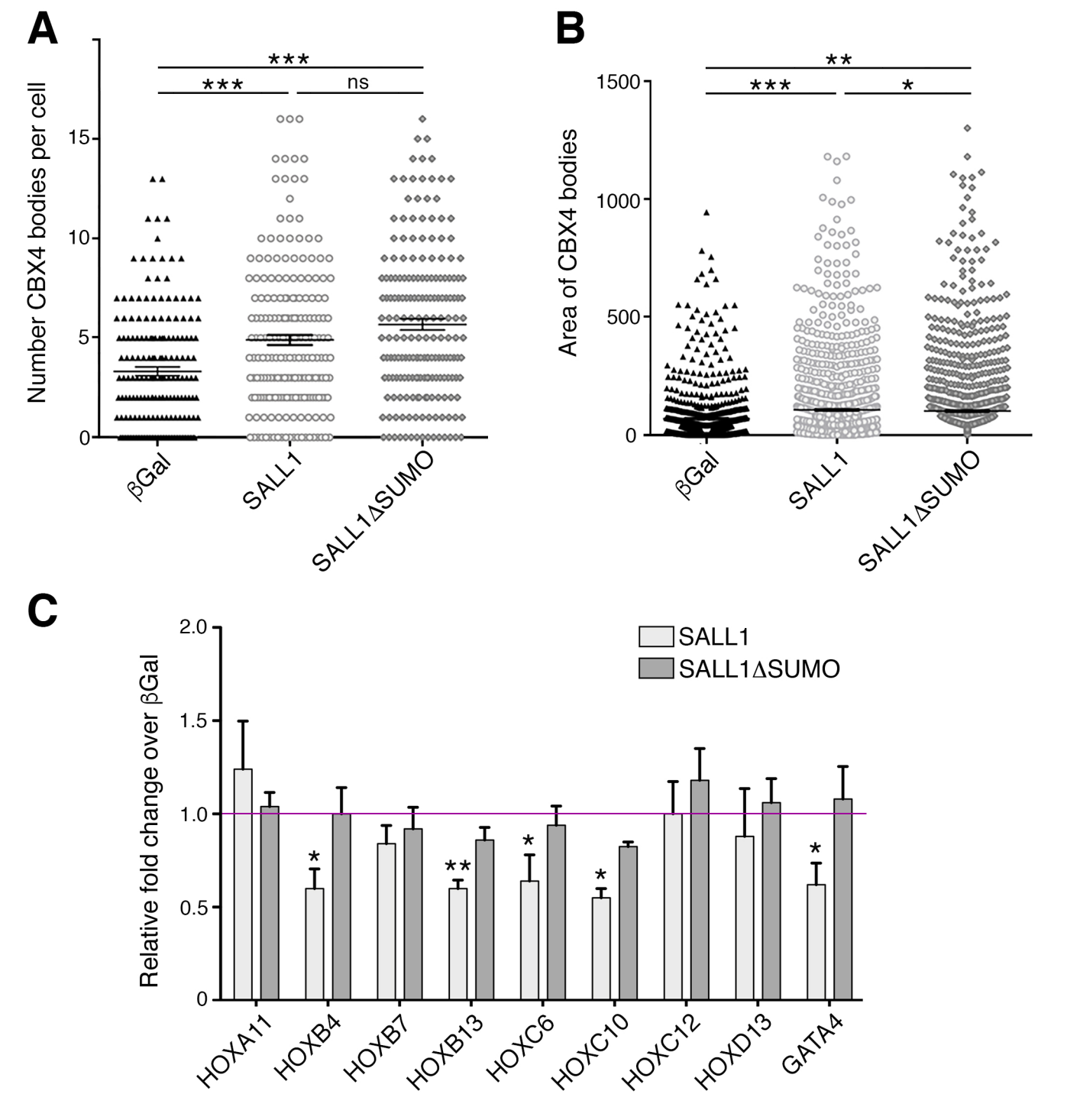
A
Number CBX4 bodies per cell
***
***
ns
0
5
10
15
βGal
SALL1
SALL1ΔSUMO
B
Area of CBX4 bodies
**
***
*
0
500
1000
1500
βGal
SALL1
SALL1ΔSUMO
C
Relative fold change over βGal
SALL1
SALL1ΔSUMO
0
0.5
1.0
1.5
2.0
HOXA11
HOXB4
HOXB7
HOXB13
HOXC6
HOXC10
HOXC12
HOXD13
GATA4

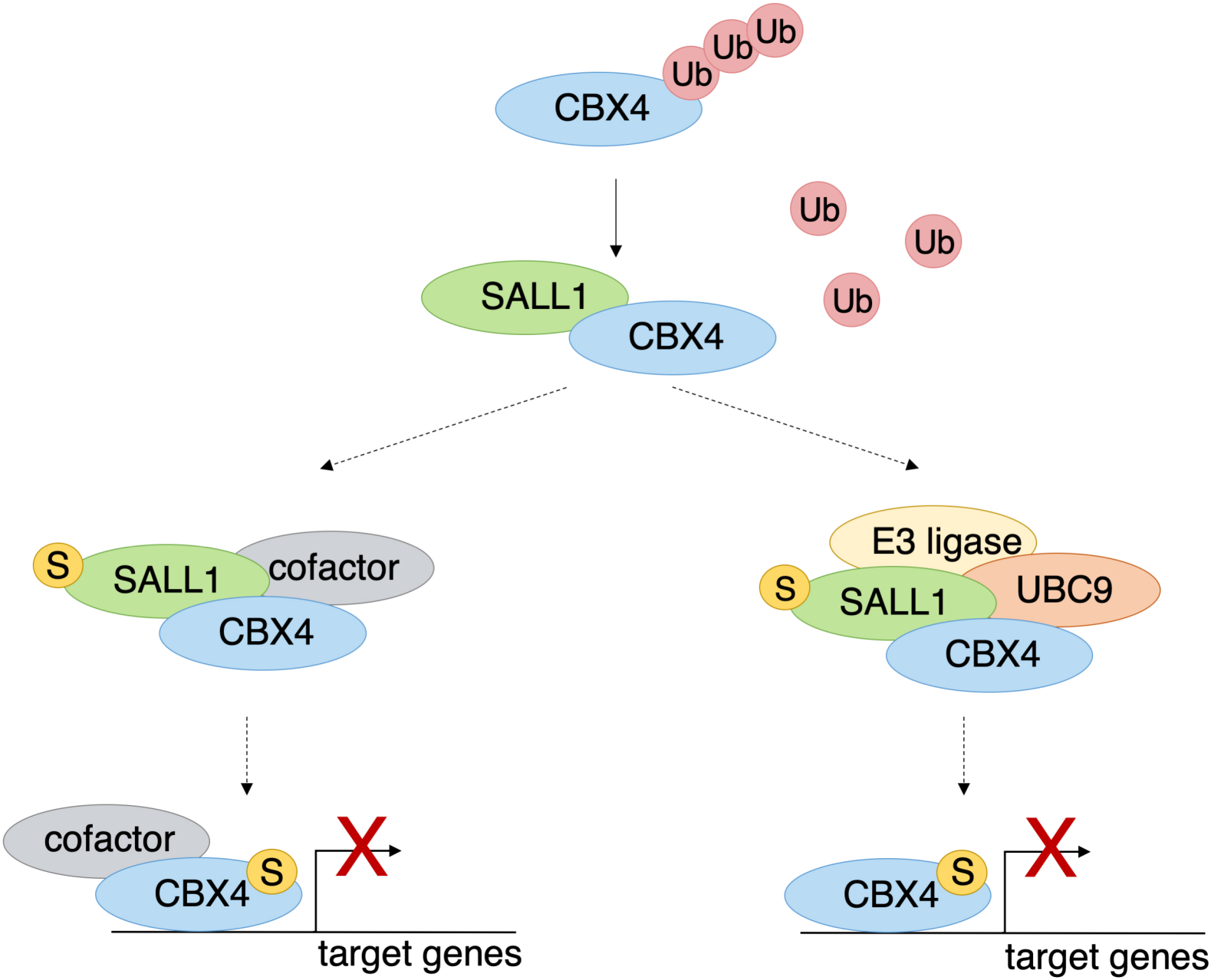
Ub
Ub
Ub
CBX4
Ub
Ub
Ub
SALL1
CBX4
S
SALL1
cofactor
CBX4
E3 ligase
S
SALL1
UBC9
CBX4
cofactor
CBX4
S
target genes
CBX4
S
target genes